

Spring 2016

# Dissolution kinetics of model api in molten polymer excipients during batch processing

Shen Ji

*New Jersey Institute of Technology*

Follow this and additional works at: <https://digitalcommons.njit.edu/theses>



Part of the [Chemical Engineering Commons](#)

---

## Recommended Citation

Ji, Shen, "Dissolution kinetics of model api in molten polymer excipients during batch processing" (2016). *Theses*. 273.  
<https://digitalcommons.njit.edu/theses/273>

This Thesis is brought to you for free and open access by the Theses and Dissertations at Digital Commons @ NJIT. It has been accepted for inclusion in Theses by an authorized administrator of Digital Commons @ NJIT. For more information, please contact [digitalcommons@njit.edu](mailto:digitalcommons@njit.edu).

## **Copyright Warning & Restrictions**

The copyright law of the United States (Title 17, United States Code) governs the making of photocopies or other reproductions of copyrighted material.

Under certain conditions specified in the law, libraries and archives are authorized to furnish a photocopy or other reproduction. One of these specified conditions is that the photocopy or reproduction is not to be “used for any purpose other than private study, scholarship, or research.” If a user makes a request for, or later uses, a photocopy or reproduction for purposes in excess of “fair use” that user may be liable for copyright infringement,

This institution reserves the right to refuse to accept a copying order if, in its judgment, fulfillment of the order would involve violation of copyright law.

**Please Note: The author retains the copyright while the New Jersey Institute of Technology reserves the right to distribute this thesis or dissertation**

Printing note: If you do not wish to print this page, then select “Pages from: first page # to: last page #” on the print dialog screen

The Van Houten library has removed some of the personal information and all signatures from the approval page and biographical sketches of theses and dissertations in order to protect the identity of NJIT graduates and faculty.

## **ABSTRACT**

### **DISSOLUTION KINETICS OF MODEL API IN MOLTEN POLYMER EXCIPIENTS DURING BATCH PROCESSING**

**by**

**Shen Ji**

In the pharmaceutical industrial application field, hot-melt extrusion (HME) has been recently introduced to develop new solid dosage forms and products. By dissolving the poorly-soluble active pharmaceutical ingredients (API) into water-soluble polymers, the bioavailability of the Class II (with low solubility and high permeability in water) API in Biopharmaceutical Classification System (BCS) could be significantly improved in the body. For readily water-soluble API, HME provides a new approach to produce a controlled release drug system. Hence, pharmaceutical HME is a promising processing method in the pharmaceutical industry.

However, HME has not been widely applied into the pharmaceutical industry. The thermal degradation of the polymer (and/or other excipients) and API are major concerns in the pharmaceutical HME process: researchers aim to dissolve the total loading of the API into the excipient within the short residence time with minimal API degradation. Therefore, the kinetics of the dissolving process should be known. In this work, the expression of dissolution process and the impact of shear rate, API concentration and API species in dissolution kinetics are determined. The viscosities of the mixture at different shear rates are also measured. A model API shall be dissolved into a polymeric excipient by conducting melt-mixing experiments using the Brabender Batch Mixer.

**DISSOLUTION KINETICS OF MODEL API IN MOLTEN POLYMER  
EXCIPIENTS DURING BATCH PROCESSING**

**by  
Shen Ji**

**A Thesis  
Submitted to the Faculty of  
New Jersey Institute of Technology  
In Partial Fulfillment of the Requirements for the Degree of  
Master of Science in Chemical Engineering**

**Otto H. York Department of Chemical, Biological and Pharmaceutical Engineering**

**May 2016**

Blank Page

**APPROVAL PAGE**

**DISSOLUTION KINETICS OF MODEL API IN MOLTEN POLYMER  
EXCIPIENTS DURING BATCH PROCESSING**

**Shen Ji**

---

Dr. Costas G. Gogos, Thesis Advisor Date  
Distinguished Research Professor of Chemical, Biological and  
Pharmaceutical Engineering, NJIT & President Emeritus of Polymer  
Processing Institute (PPI)

---

Dr. Reginald P. Tomkins, Committee Member Date  
Professor of Chemical, Biological and Pharmaceutical Engineering, NJIT

---

Dr. Laurent Simon, Committee Member Date  
Associate Professor of Chemical, Biological and Pharmaceutical Engineering, NJIT

---

Dr. Nicholas Ioannidis, Committee Member Date  
Research Engineer of Polymer Processing Institute

## **BIOGRAPHICAL SKETCH**

**Author:** Shen Ji  
**Degree:** Master of Science  
**Date:** May 2016

### **Undergraduate and Graduate Education:**

- Master of Science in Pharmaceutical Engineering,  
New Jersey Institute of Technology, Newark, NJ, USA, 2016
- Bachelor of Engineering in Pharmaceutical Engineering  
Yunnan University, Kunming, Yunnan, P. R. China, 2013

**Major:** Chemical Engineering



I dedicate this thesis to my beloved parents,

Junying Wu and Yanping Ji.

It is their love, support and comprehension that make me who I am.

献给我挚爱的父母，

吴俊英和季延平

是他们的爱、支持和理解造就了我

## **ACKNOWLEDGMENT**

I am extremely thankful to Prof. Costas Gogos, who as my advisor, provided me with valuable resources, gave me brilliant academic guidance, as well as the courage and confidence to overcome issues I encountered throughout my Master's studies. It is a great privilege and honor for me to have received his advice.

I would also like to thank Dr. Nicolas Ioannidis for his hard work, patient instructions and kindly support throughout my thesis work. Special thanks are given to Prof. Reginald Tomkins and Prof. Laurent Simon for their participation in my thesis committee.

I am also highly thankful to The Polymer Processing Institute (PPI) located at NJIT for making their facilities available to me, and the advice and help I received from the other staff. I also want to thank Dr. Chunmeng Lu, Dr. Herman Suwardie and Mr. Huayang Fang for their generous help.

Finally, I give my deepest gratitude to my parents, Junying Wu and Yanping Ji. Their love and support gave me endless energy and the spirit to make this thesis possible.

## TABLE OF CONTENTS

| <b>Chapter</b> |  | <b>Page</b> |
|----------------|--|-------------|
| 1              | INTRODUCTION.....  | 1           |
| 1.1            | Objective.....   | 2           |
| 1.2            | Background Information.....  | 2           |
| 1.2.1          | Hot-melt Extrusion.....  | 2           |
| 1.3            | Distributive Mixing and Dispersive Mixing.....   | 5           |
| 1.4            | Dissolution of API Particles in Polymeric Melt.....  | 6           |
| 1.5            | Viscosity of the Melt.....   | 11          |
| 2              | MATERIALS AND METHODS.....   | 13          |
| 2.1            | Materials.....   | 13          |
| 2.2            | Methods.....   | 14          |
| 2.2.1          | Batch Mixer.....   | 14          |
| 2.2.2          | Light Microscopy.....  | 18          |
| 2.2.3          | Rheometric Mechanical Spectrometer.....  | 18          |
| 3              | RESULTS AND DISCUSSION.....  | 19          |
| 3.1            | API Particle Dispersion, Distribution, and Dissolution in the Molten<br>Polymer Excipient..... | 19          |

**TABLE OF CONTENTS**  
**(Continued)**

| <b>Chapter</b>   | <b>Page</b> |
|--|-------------|
| 3.1.1 The Set Temperature.....   | 19          |
| 3.1.2 Dispersion and Dissolution.....  | 20          |
| 3.2 Dissolution of the API at Different Shear Rate.....                        | 23          |
| 3.2.1 Shear Rate.....  | 23          |
| 3.2.2 Exponential Decay.....   | 24          |
| 3.2.3 Drugs Concentration Effect.....  | 29          |
| 3.2.4 Effect of API Species.....   | 31          |
| 3.2.5 The Viscosity of the API/Excipient Systems at Different Shear Rates..... | 33          |
| 4 SUMMARY, CONCLUSION AND FUTURE WORK.....                                     | 41          |
| 4.1 Summary.....   | 41          |
| REFERENCES.....  | 44          |

## LIST OF FIGURES

| <b>Figure</b> |   | <b>Page</b> |
|---------------|---|-------------|
| 1.1           | Dispersive mixing and distributive mixing of solid agglomerates and immiscible liquid droplets.....                                     | 5           |
| 1.2           | Schematic representation of the morphological changes of the drug and polymer system in the solution formation process for Case I.....  | 7           |
| 1.3           | Schematic representation of the morphological changes of the drug and polymer system in the solution formation process for Case II..... | 8           |
| 2.1           | The batch mixer (a) and roller screws (b) (Manufactured by Brabender Corp.).....  | 15          |
| 2.2           | The inside of the assembled Brabender batch mixer (without the front plate).....  | 16          |
| 2.3           | Torque vs time measured by old load cell.....   | 17          |
| 2.4           | Data comparison between two load cells.....   | 17          |
| 3.1           | Melt temperature at different screw speed.....  | 20          |
| 3.2           | 96%EPO-4%APAP vs. 100%EPO control.....  | 21          |
| 3.3           | Viscosity ratios of suspensions and viscosity ratios of suspended drug particles in molten polymer matrix.....                          | 22          |
| 3.4           | Cartoon representation of the dissolution of APAP in molten EPO.....  | 23          |
| 3.5           | Averaged torque traces with normalized time.....  | 25          |
| 3.6           | Exponential decay curves after normalization.....   | 25          |
| 3.7           | $C_1$ vs RPM.....   | 27          |
| 3.8           | $C_2$ vs RPM.....   | 27          |
| 3.9           | $\tau_0$ vs RPM.....  | 28          |

**LIST OF FIGURES**  
**(Continued)**

| <b>Figure</b> |   | <b>Page</b> |
|---------------|---|-------------|
| 3.10          | Torque trace at 50RPM & 100RPM.....         | 30          |
| 3.11          | APAP particles and QTP particles.....       | 31          |
| 3.12          | Torque trace of APAP and QTP at 100RPM..... | 32          |
| 3.13          | Rheology results.....                       | 33          |

## LIST OF TABLES

| <b>Table</b>  | <b>Page</b> |
|---|-------------|
| 3.1 Set Temperature at Different Screw Speed.....                                   | 19          |
| 3.2 Exponential Decay Model Parameters for 4%APAP at Different RPM...               | 26          |
| 3.3 Exponential Decay Model Parameters for Different Condition and Formulation..... | 29          |
| 3.4 Exponential Decay Model Parameters for Different API.....                       | 32          |
| 3.5 Dynamic Viscosities at Given Shear Rates.....                                   | 36          |
| 3.6 Calculation of " $\gamma_i \times \eta_i$ ".....                                | 37          |
| 3.7 Solubility Parameter Calculations of EPO.....                                   | 38          |
| 3.8 Solubility Parameter Calculations of APAP.....                                  | 38          |
| 3.9 Solubility Parameter Calculations of QTP.....                                   | 39          |

# CHAPTER 1

## INTRODUCTION

### 1.1 Objective

Hot-melt extrusion, as an evolving, continuous and solvent-less polymer processing method, has been recently adopted by the pharmaceutical industry to prepare solid oral dosage formulations with increased bioavailability for the poorly-water soluble drugs and controlled release characteristics for the water-soluble drugs (Maniruzzaman, Boateng et al. 2012). In the case of poorly water-soluble drugs, bioavailability enhancement is achieved through amorphization of the crystalline drug, such like BCS class II active pharmaceutical ingredients (APIs). Utilizing HME can improve the bioavailability of the poorly water-soluble APIs by dissolving them in to water-soluble polymers. Specific intermolecular bonds with, and steric hindrance effects by the polymer chain prevent the drug from re-crystallizing. Although the extrusion process during the production of solid solutions typically takes place below the melting point of the drug, the potential of thermal degradation of the API still exist and may in fact be a major concern preventing the universal applicability of the HME technique as a pharmaceutical manufacturing method. To completely dissolve the API in the formulation while minimizing its potential thermal degradation, the dissolution kinetics of the API into the excipient must be known. In the dissolution process, shear rate dependent viscosity is an important material variable: shear rate can be estimated with a given screw speed and the dimensions of the instruments; viscosity shall be estimated using the RMS rheometer. Additionally the species, which is the chemical structure of the API particle also affects the dissolving rate. In this work, we



determine the dissolution kinetics of a model API into a polymeric excipient by conducting melt-mixing experiments with a Brabender Batch Mixer.

## **1.2 Background Information**

### **1.2.1 Hot-melt Extrusion**

Hot-melt extrusion has been used in the plastic, rubber, and food manufacturing industry to produce items such as pipes, sheets, and bags. And it has emerged as a novel processing technology in developing oral dosage molecular dispersions (solid solutions) of poorly water-soluble APIs into various hydrophilic polymer matrices. The Hot-melt extrusion technology has proven to be a robust method of producing numerous drug delivery systems, and therefore, it has been found to be useful in the pharmaceutical industry as well (Andrews, 2010; Crowley, 2007). HME involves the compaction and conversion of blends from a powder or a granular mix into a product of uniform shape (Breitenbach, 2002). During this process, polymer are melted and formed into products having different shapes and sizes such as tablets, capsules, films, and implants for drug delivery. The extrusion process can be broken down to the following general process sections (Chokshi et al. 2004):

- (1) Feeding of the extruder by a hopper;
- (2) Mixing, grinding, reducing the particle size, and kneading;
- (3) Flow through the die;
- (4) Extrusion from the die and further downstream processing.

Noticeably, HME can improve the bioavailability of the poorly water-soluble active pharmaceutical ingredients by dissolving them into water-soluble polymers. At the same time, oral dosages with controlled release characteristics can be produced by

dispersing water-soluble APIs into water-insoluble polymers. The elementary steps of this process are identical to the ones involved in conventional plastics melt compounding by extrusion: (1) Feeding particulates; (2) melting; (3) dispersive and distributive mixing; (4) devolatilization and stripping; (5) pressurization and pumping. However, for pharmaceutical hot-melt extrusion, the API dissolution is an additional and very important elementary step, along with melting of the polymeric excipient that precedes it, and mixing which accelerates the dissolution process. In the case of solid solutions, the drug's (API) dissolution is an additional and very important elementary step, along with melting of the polymeric excipient that precedes it, and mixing which accelerates the dissolution process.

HME provides several advantages over traditional available pharmaceutical processing techniques such as (1) Increased solubility and bioavailability of water-insoluble compounds; (2) solvent free process; (3) economical process with reduced production time, fewer processing steps, and a continuous operation; (4) capabilities of sustained, modified, and targeted release; (5) better content uniformity in products; (6) no needs for the compressibility of active ingredients; (7) uniform dispersion of fine particles; (8) good stability at changing pH and moisture levels and safe application in humans; (9) reduced number of unit operations and production of a wide range of performance dosage forms; (10) a range of screw geometries (McGnity et al. 2004),( Jones et al. 2008), (Grunhagen et al. 1995), (Singhal et al. 2011). However, the HME also have disadvantages as well. The main drawbacks of HME include thermal process (drug/polymer stability), use of high viscosity polymers, and excipients required and not suitable for relatively high temperature sensitive molecules such as microbial species and proteins (Grunhagen et al. 1995), (Singhal et al. 2011), and the newer class of drugs called “biologics”.

As mentioned previously, the thermal degradation of drugs (API) is one of the major concern in pharmaceutical HME process. Producing an extrudate that contains a molecularly dissolved API and at the same time not overexposing the API to high processing temperature for inappropriately long time is one of the major objectives during the extrusion of solid solutions. To achieve the balance between complete dissolution of API and minimal thermal degradation of the API, the dissolution kinetics of the API particulates inside the molten polymeric matrix during extrusion must be known. Melting of the polymeric excipient, dispersive/distributive mixing, and API dissolution can occur simultaneously during extrusion. Therefore, to determine the dissolution kinetics of API, the above phenomena must be isolated from each other. One way to achieving this is by exploiting the effect of polymer melting, dispersion and distribution of API particulates and API dissolution on the melt viscosity of the polymer matrix: melt viscosity decreases with increasing temperature. Addition of particulates in molten polymers may increase the melt viscosity. Dissolution of an API into molten polymers as a rule decreases viscosity by virtue of the plasticizing action of the small particles.

In this work, we determine the impact of shear rate and API species on dissolution kinetics of API into Eudragit®E PO by performing batch melt-mixing experiments using a specific following protocol: first we melt-mix the polymer and allow it to reach steady state, then add the crystalline API quickly and in small quantities. In this way, we minimize the effect of dispersion and distribution that occurs prior to and during the dissolution of the API. Following the addition of the API to the molten polymer, the dissolution kinetics are then determined from the drop in the torque of the processed formulation by virtue of the API plasticization of the polymer.

### 1.3 Distributive Mixing and Dispersive Mixing

The mixing processes in single or twin screw extruders is induced by laminar flow and is generally categorized into two types: dispersive mixing and distributive mixing. Dispersive mixing refers to the process involving the laminar flow stress-induced particle size reduction (i.e. de-agglomeration) of particulate cohesive components such as fillers, polymer gels, or liquid droplets. Distributive mixing refers to increasing and stretching the interfacial area between the components lacking a cohesive force in between and distributing them uniformly throughout the volume of the molten polymer. Dispersive mixing is mainly controlled by the laminar shear or extensional forces and distributive mixing is mainly controlled only by the flow-generated strains and does not require high stresses. According to the definitions, the mixing of miscible liquids is regarded as distributive mixing, and mixing of hard solid agglomerates, immiscible liquids, and soft agglomerates is regarded as dispersive mixing (Tadmor, Gogos, 2006). The dispersive and distributive mixing of solid agglomerates is schematically shown in Figure 1.1.

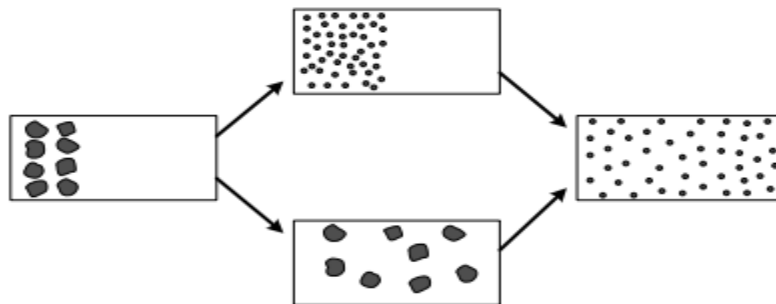


**Figure 1.1** Dispersive mixing and distributive mixing of solid agglomerates and immiscible liquid droplets (Tadmor and Gogos, 2006).

Source: Z. Tadmor, C. G. Gogos (2006). *Principles of Polymer Processing*, John Wiley & Sons, Inc. Hoboken, NJ, USA.

### **1.4 Dissolution of API Particles in Polymeric Melt**

The dissolution of API within the polymer largely depends on their physicochemical properties. Good blended dispersions require miscibility between the drug and polymer (Marsac, 2009). In practice, the majority of drug/polymer systems cannot show fully miscibility, they may likely to show only partial miscibility. This means that there exists a certain thermodynamic solubility of drugs in polymer matrixes. HME can be carried out in two distinctly different conditions, referred to here as Case I and Case II:

Case I: The processing temperature is above the melting temperature for a semi-crystalline polymer, or the softening temperature for an amorphous polymer, ( $T_g + 50 \sim 100 \text{ }^\circ\text{C}$ ) but below the melting point of a drug.

Case II: The processing temperature is above both the melting temperature and the softening temperature of semi-crystalline or amorphous polymers, respectively, and above the melting point of a drug. It is important to be noted that processing temperature should be the melt temperature instead of the set temperature of the processing equipment. It should also be noted that the glass transition temperature of an amorphous polymer or the melting temperature of a semi-crystalline polymer may decreased if incorporation of the API (Crowley et al. 2007).

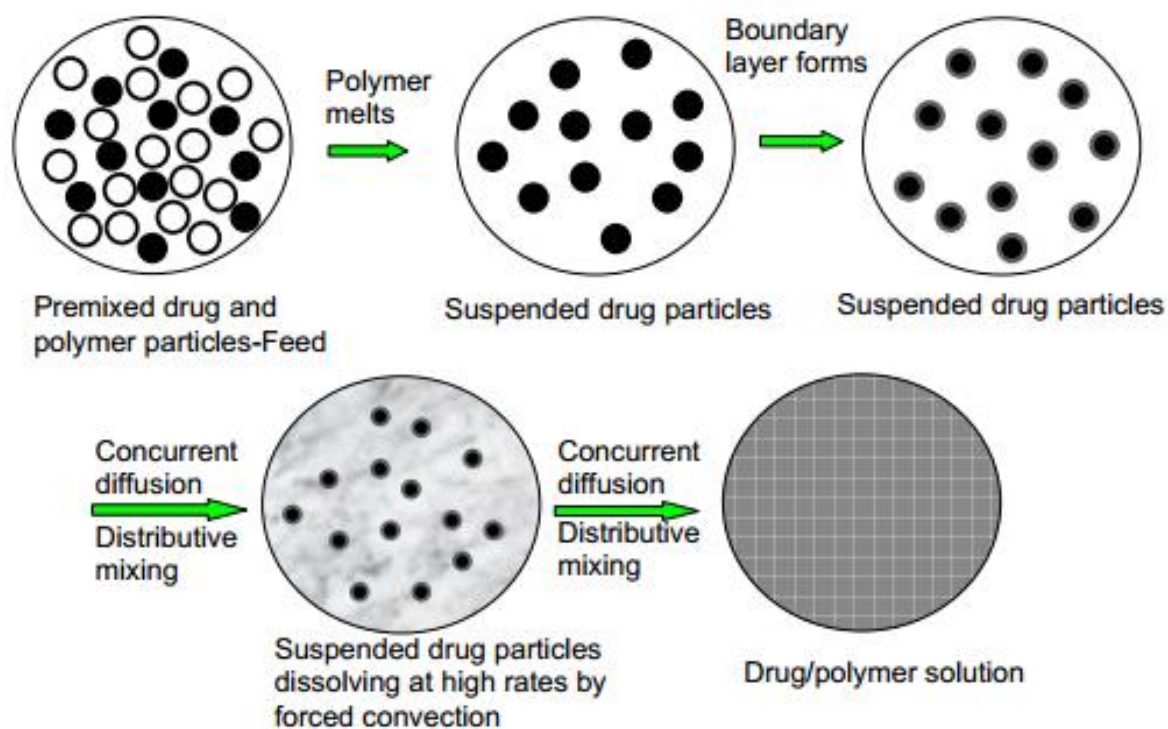


**Figure 1.2** Schematic representation of the morphological changes of the drug and polymer system in the solution formation process for Case I.

Source: C.G. Gogos, H. Liu, P. Wang, in: Douroumis, *“Hot-Melt Extrusion: Pharmaceutical Applications,”* Wiley: Chichester, UK, 2012.

Case I provides a viable method to circumvent the thermal degradation issues. In Case I, the drug is processed below its melting point and mixed with a polymer melt, then the solid drug particles gradually dissolve into the polymer excipient melt. And this process should be able to provide a desirable polymer-drug solid dispersion or solid solution. During the HME process, the solid API act as a solute and the polymeric melt act as a solvent. In addition, the dissolution rate and solubility of the API in the polymer will increase with higher temperature.

The dissolution process of the drug in the polymer melt is schematically shown in Figure 1.2. Firstly, the drug particles (black) and polymer particles (white) are fed into

the batch mixer or an extruder. Secondly, the polymer particles start melting due to the conductive heat from the mixer or extruder barrel and frictional and plastic energy dissipation. These two phenomena result in a process charge state that the solid drug particles are suspended in a continuous polymer melt matrix. Thirdly the polymer molecules start to heat up the API particles and create a mass transfer boundary layer. This layer shall be continuously wiped away and replaced with fresh polymer melt nearby. The drug molecules diffuse into the polymer melt through the boundary layer, and the size of the suspended drug particles will continue to decrease as the diffusion goes. Finally, a homogeneous *solution* will be formed.

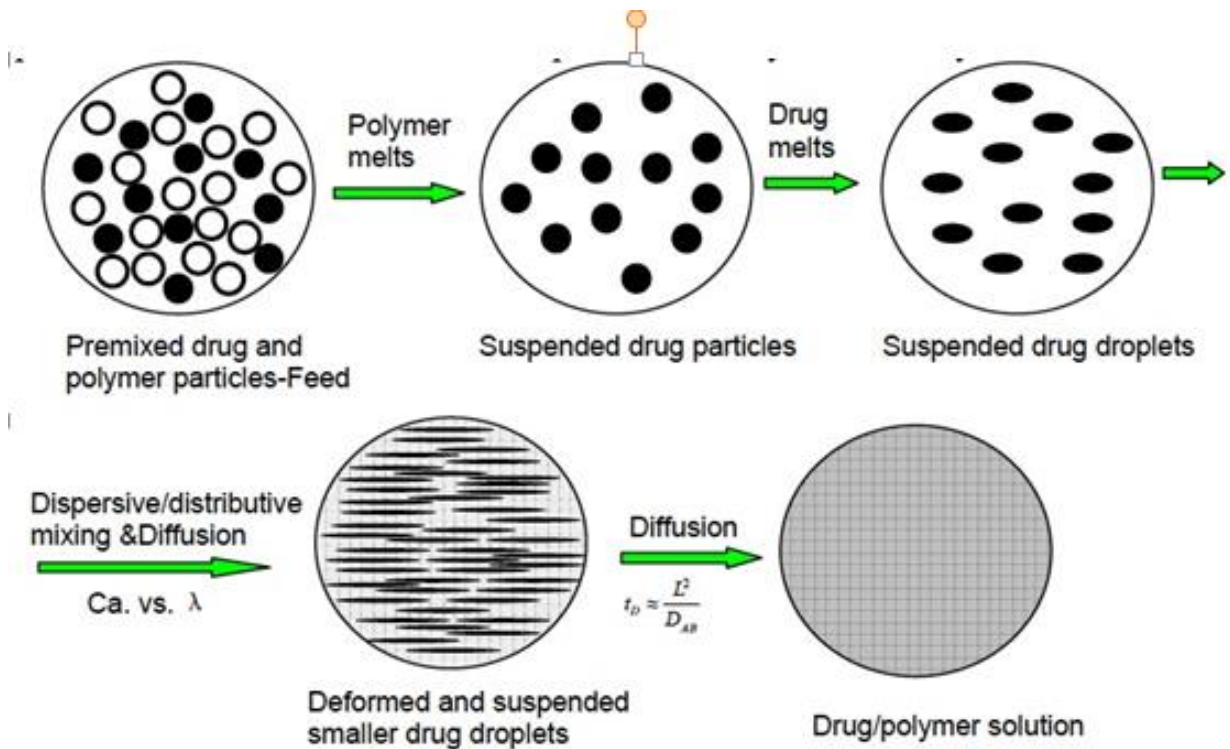


**Figure 1.3** Schematic representation of the morphological changes of the drug and polymer system in the solution formation process for Case II.

Source: C.G. Gogos, H. Liu, P. Wang, in: Douroumis, "Hot-Melt Extrusion: Pharmaceutical Applications," Wiley: Chichester, UK, 2012.

Case II, on the other hand, involves miscible or partially miscible liquid-liquid mixing because both the polymer and drug will be melted. As shown in Figure 1.3, the drug (black) and polymer (white) particles are fed into an extruder and processed by the screw elements. Due to the heat transfer from the extruder barrel or a batch mixer, and frictional and plastic dissipation, the polymer particles will melt first. During or after the melting of the polymer, the drug particles will melt to droplets and be deformed by the mixing flows generated by the screws. The droplets will be deformed along the shear direction and blurred the contacting surface between the drug and polymer. As this process goes on and with diffusion continuously being carried on, we will finally get a homogeneous drug – polymer solution.

In both cases discussed previously between either the dissolving API particles or the drug droplets and the molten polymer, the diffusion will happen. The “characteristic diffusion time”  $t_D$  is proportional to the square of the API phase droplet or ligament radius  $L$  or the thin dimension.  $D_{AB}$  is the diffusivity of the API into the polymer melt excipient. They are related by the following useful expression, Equation 1.1.

$$t_D = \frac{L^2}{D_{AB}} \quad (1.1)$$

During the HME process, the relationship between the rate of dissolution of drug particles in molten polymer excipients,  $dm/dt$ , and the solubility,  $C_s$ , is described by the Noyes-Whitney expression, Equation 1.2, as follows:

$$\frac{dm}{dt} = \frac{D \times A \times (C_s - C)}{h \times V} \quad (1.2)$$

where  $m$  = mass (mol),  $t$  = time (s),  $C$  = concentration of solute dissolved at a particular time ( $\text{mol} \cdot \text{cm}^{-3}$ ),  $C_s$  = equilibrium solubility ( $\text{mol} \cdot \text{cm}^{-3}$ ),  $D$  = diffusivity ( $\text{cm}^2 \cdot \text{s}^{-1}$ ),  $h$  =



apparent thickness (cm) of the aqueous boundary layer (depends on rate of stirring and the temperature), and A = surface area available for dissolution (cm<sup>2</sup>).

The equation indicates that the drug particle size and size distribution are important variables to affect the dissolution rate, because the total contacting surface area of the drug particles will be changed correspondingly. A higher dissolution rate is expected with smaller particles. Furthermore, the narrower the drug particle size distribution, the more uniform the total dissolution time distribution needed for complete dissolution of drugs in polymer melt will be (Liu, Gogos, 2012). Also, the diffusivity, which determined by temperature and the property of the particle, plays a significant role in dissolution process. At some constant temperature, for particles with similar sizes or at same size scale, the particles with higher diffusivity are expected to have shorter diffusion time. This may lead to a method to evaluate the diffusive property of the particles (Fang, 2014).

Process parameters have an important impact on the dissolution rate of drug particulates in polymeric melts. For co-twin screw extruders, the most important process parameters are the barrel set temperature, the screw speed and the feeding rate. Screw speed can be used to calculate the “characteristic average” channel shear rate and shear stress:

$$\gamma = \frac{\pi \times D \times n}{h \times 60} \quad (1.3)$$

$$\tau = \gamma \times \eta \quad (1.4)$$

where  $\gamma$  is shear rate in sec<sup>-1</sup>; D is the screw diameter in mm; n is the screw speed in rpm; h is the over-flight clearance in mm;  $\tau$  is shear stress in kPa;  $\eta$  is the melt viscosity in Pa\*s (Gogos, Liu, Wang, 2012). According to Equation (1.3), for a given extruder, once the screw speed is fixed, the characteristic shear rate is a constant value.

In order to raise the dissolution rate, the surface area available have to be consider. In extrusion process, the dispersive mixing may break up the drug agglomerates or individual particles due to the high shear forces generated by the high shear screw elements such as wide kneading blocks or Maddock elements (Tadmor, Gogos, 2006). Then, the total contacting surface area of the drug particles to the polymeric melt will be larger, thus the dissolution rate will increase. And the distributive mixing can homogenize the drug concentration dissolved in the polymeric melt, and leading more polymer melt into contact with the suspended drug particles. In this way, both effects can raise or maintain the dissolution rate. Thus, it is expected that with higher shear rate, the dissolution rate would rise, which could be accomplished through increasing the screw speed of an extruder.

If the mixer set temperature increases, on the one hand, the diffusion coefficient will increase due to the increased temperature and resultant decreased matrix viscosity; on the other hand,  $C_s$  also will increase. Both of these factors will contribute to an increase of the API dissolution rate in the molten polymer excipient. As the screw speed increases, the distributive mixing is improved within the chamber as well, and thus a higher concentration gradient around the drug particulates is available. Moreover, the thickness of the mass transfer boundary layer decreases as the screw speed increases. Both effects contribute to an increased dissolution rate.

### **1.5 Viscosity of the Melt**

The temperature dependent viscosity of a polymer in its molten state affects the melt extrusion process: the level of temperatures reached because of viscous energy dissipation, the melting rate, the die flow uniformity and extrudate quality. Polymers with high

viscosities generate higher melt temperatures and higher melting rates in the screw. They also require die discharge pressure and more power. For different polymer-drug formulations, the viscosity of the mixture also varies. The viscosity of the polymers are determined by a rheometric mechanical spectrometer (Nollenberger and Albers, 2012). According to Equation (1.3), given the screw speed and the dimension of the barrel and the rotors, the characteristic channel shear rate could be calculated, but the shear stress and the viscosity cannot be directly determined independently by the batch mixer: only the overall torque could be recorded continuously during the evolution of the batch process of polymer melting, dispersive and distributive mixing of the API as well as the API dissolution process. In this work, the viscosity of the material at different shear rate was measured independently to find a relationship between the apparent torque and the viscosity of the melt mixture.

## CHAPTER 2

### MATERIALS AND METHODS

#### 2.1 Materials

Eudragit® E is a copolymer composed of neutral methyl and butyl methacrylate, and dimethylaminoethyl methacrylate repeating units. It has a  $T_g \sim 45^\circ\text{C}$ . The molar ratio of three monomers, methyl methacrylate, butyl methacrylate and dimethylaminoethyl methacrylate, is 2:1:1. Two grades are available which have the same chemical structure and molecular weight: one is Eudragit® E PO (EPO) in powder form; the other is Eudragit® E 100 in granular form. This copolymer is soluble up to pH=5 and above this pH value is capable of swelling and becoming permeable to water. It is widely used for masking unpleasant tastes and odors of drugs, protecting drugs against moisture, and as a drug excipient for pharmaceutical applications. In this work, EPO is selected as the model polymer excipient.

Acetaminophen (APAP) (Spectrum Chemicals, Gardena, CA) was selected as one of the model crystalline API. APAP is a water-soluble BCS class I drug with a  $T_m$  of 169–170 °C.

Quetiapine is select as another model API in this work. Quetiapine is an atypical antipsychotic which has a dibenzothiazepine structure. The  $T_m$  of quetiapine fumarate is 174~175 °C (Gohel and Patel, 2013). Due to its poor solubility over the physiological pH range and high permeability, quetiapine is classified as a BCS class II drug. Quetiapine is available as fumarate salt in immediate release and extend release formulations (Grzegorz Garbacz, et al. 2013). In this work, quetiapine fumarate is used in the experiments and QTP

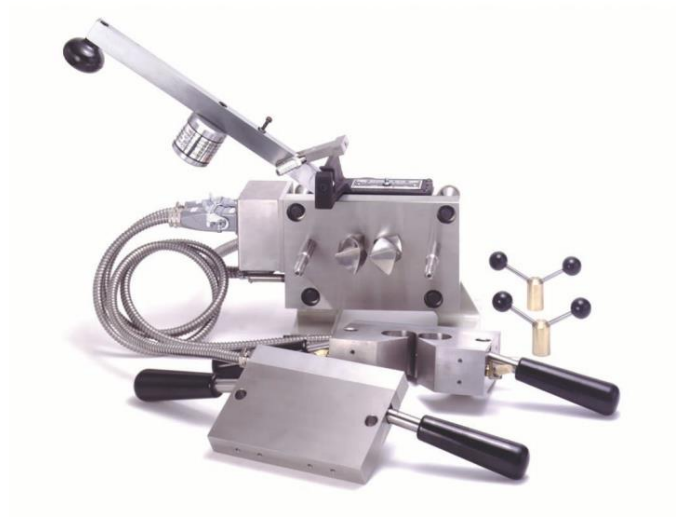
represents quetiapine fumarate in the rest of the content.

## **2.2 Methods**

### **2.2.1 Batch Mixer**

A batch mixer is used to experimentally investigate the effects of extrusion process parameters (torque and melt temperature) of the drug-polymer mixing. The batch mixer is a heated high-shear laminar-flow mixer, which has been extensively used in the plastics and rubber industry to simulate the extrusion process, reactive extrusion, or optimize the formulation. The laboratory scale batch mixer used requires only 30-60 g of the material and many experiments can be performed in a short period of time, thus making it an attractive choice for the HME study (Ghebre-Sellassie and Martin, 2007). Furthermore, the screw speeds can be controlled separately without altering the residence time in a batch mixer, which is difficult to realize if an extruder is used.

All the runs were performed in a Brabender FE-2000 batch intensive mixer utilizing counter-rotating screws, as illustrated in Figure 2.1. The batch mixer barrel is heated electrically and cooled by air. The melt temperature sensor measures the actual processed material temperature during melting and mixing; the torque meter can record the resistance of material to the flow created by the counter-rotation of the screws. Generally, about 70-75 vol. % fill degree of the chamber is recommended for good mixing because the resulting “folding” of the free surfaces is beneficial to distributive mixing. The free volume in the mixing chamber is 60 ml.



(a)



(b)

**Figure 2.1** The batch mixer (a) and roller screws (b) (Manufactured by Brabender Corp.)  
Source: Liu, H. (May 2010). Hot Melt Mixing/Extrusion and Dissolution of Drug (Indomethacin) in Acrylic Copolymer Matrices. Otto H. York Department of Chemical, Biological and Pharmaceutical Engineering. Newark, New Jersey Institute of Technology. Ph.D. Dissertation.

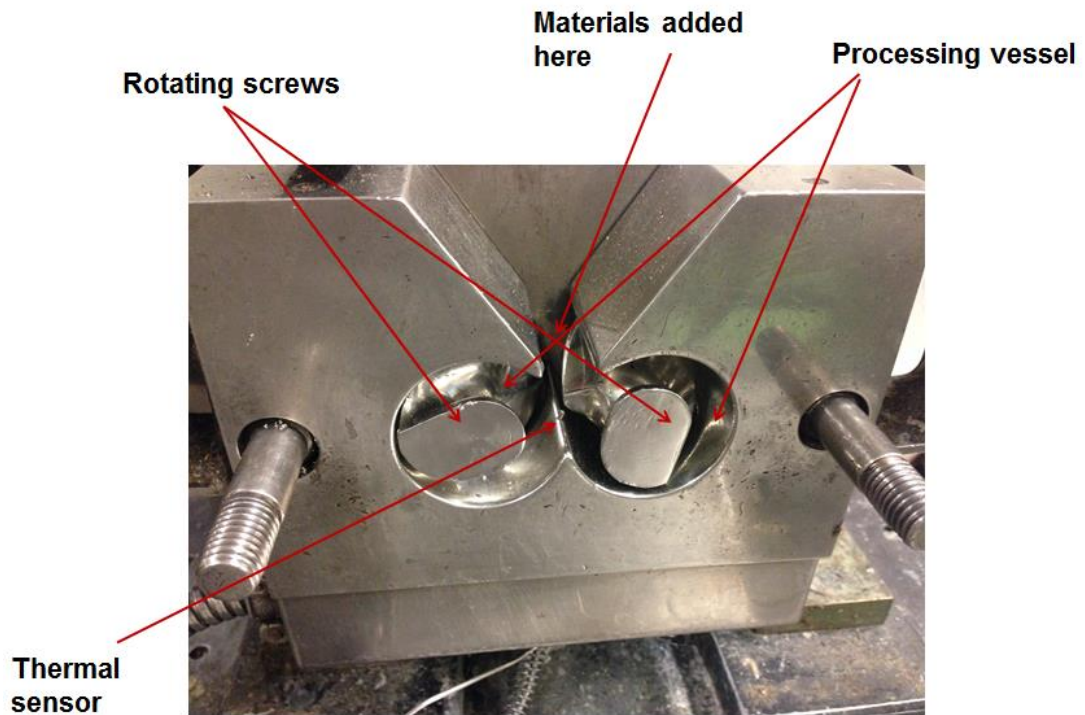


**Figure 2.2** The inside of the assembled Brabender batch mixer (without the front plate).

The Brabender batch mixer (Shown as Figures 2.1 and 2.2) was used for compounding of the materials. All the experiment runs were performed in a Brabender FE-2000 batch intensive mixer utilizing  $\Sigma$ -counter-rotating screws, as illustrated in Figure 2.1(b). During mixing, the torque arising from the resistance of material to the frictional forces while the charges in solid particulate form and later after melting, viscous flow created by the counter-rotation of the screws is recorded along with the melt temperature.

In this research work, the torque sensor lost its sensitivity, so much so that the torque at low screw speed could not be measured (for example, 25RPM, Shown as Figure 2.3). In this situation, the load cell was replaced while the new load cell isn't compatible with the original measurement program. To measure the torque of the melting mixture, the

new load cell was connected with a control box to read and record data. Calibration of the load cell was conducted before the experiment. After the change of instrument, the data recorded by the new load cell compared with previous one is shown as Figure 2.4.

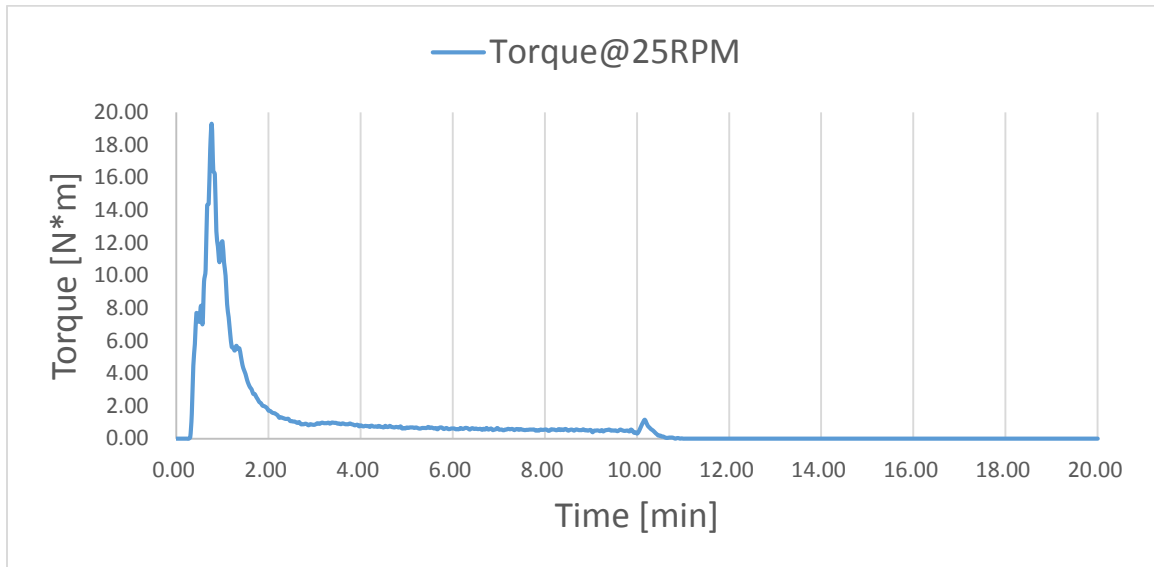


**Figure 2.3** Torque vs time measured by old load cell.

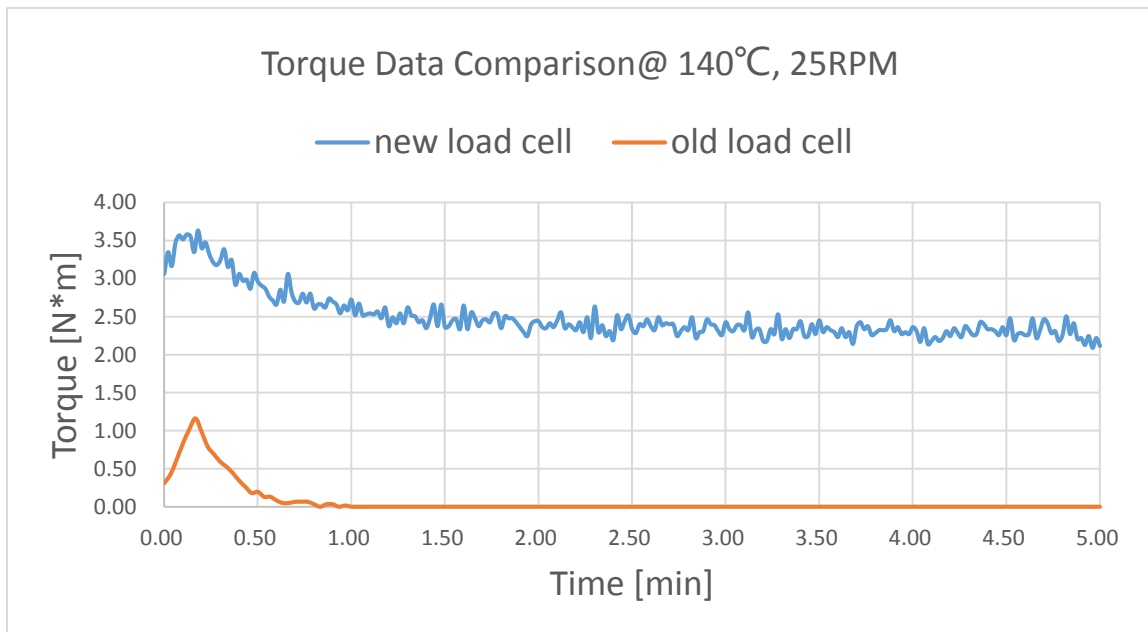


**Figure 2.4** Data comparison between two load cells.



As shown in Figure 2.2 and 2.3, the new load cell has better sensitivity of the torque but with much higher “noise”. The noise may arise from the lack of signal smoothing electronic program.

To minimize the influence of the temperature, the set temperature is selected before the mixing experiment. The melt temperature is set at 140 °C. In this work, for a given screw speed, the set temperature was set at 140°C first, then was lowered to keep the resulting melt temperature at 140°C 10min after loading the pure polymer.

All the materials were mixed at different screw speed for 20 min, while the set temperature of the mixer was shown as Table 2.1. The polymer was processed for 10 minutes before the drug was added.

### **2.2.2 Light Microscopy**

To determine the impact of the different APIs, “VHX-5000” light microscopy is used to approximately evaluate the particle size of two drugs selected in this work.

### **2.2.3 Rheometric Mechanical Spectrometer (RMS)**

RMS-800 is used to determine the viscosity of the mixture at different shear rates. The plate diameter is 25mm and the gap is ~1.2mm.

## CHAPTER 3

### RESULTS AND DISCUSSION

#### 3.1 API Particulate Dispersion, Distribution, and Dissolution in the Molten Polymer Excipient

##### 3.1.1 The Set Temperature

To determine the impact of shear rate on dissolution, the impact of melt temperature shall be eliminated. For the mixture in the batch mixer during melt processing, due to the viscous dissipation, the melt temperature is higher than the set temperature. Besides the different screw speeds result in different shear rate and shaft work, which also have different impacts on the flowing melt average temperature rise. The Brabender barrel set temperatures for different screw speeds are found as Table 3.1 shown in Materials and Methods as well as the actual resulting temperature traces shown in Figure 3.1.

**Table 3.1** Set temperature at different screw speed

| <b>RPM</b> | <b>Set Temperature /°C</b> |
|------------|----------------------------|
| 25         | 135                        |
| 50         | 132                        |
| 75         | 127                        |
| 100        | 122                        |

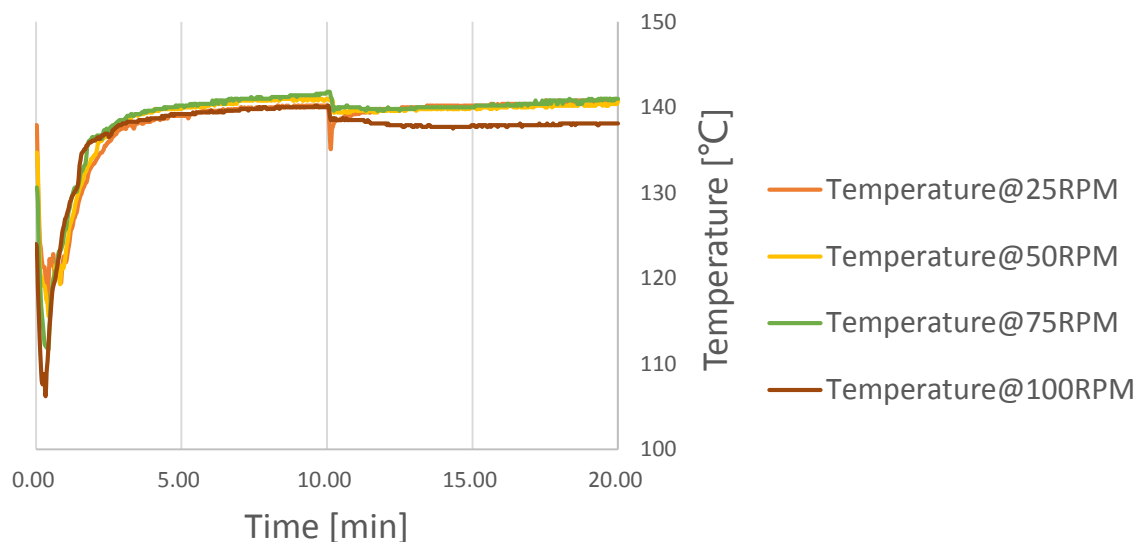


**Figure 3.1** Melt temperature at different screw speed.

Shown as Figure 3.1, from the point that the drug was added to the end point, the melt temperature at different conditions was kept at 140°C, which makes sure that the impact of temperature is fixed for all the conditions.

### 3.1.2 Dispersion and Dissolution

To determine the characteristic constants that describe the dissolution kinetics of an API in a molten polymeric excipient, the API was melt-mixed in the polymer matrix at different screw speeds and set temperatures following the addition protocol mentioned in Materials and Methods.

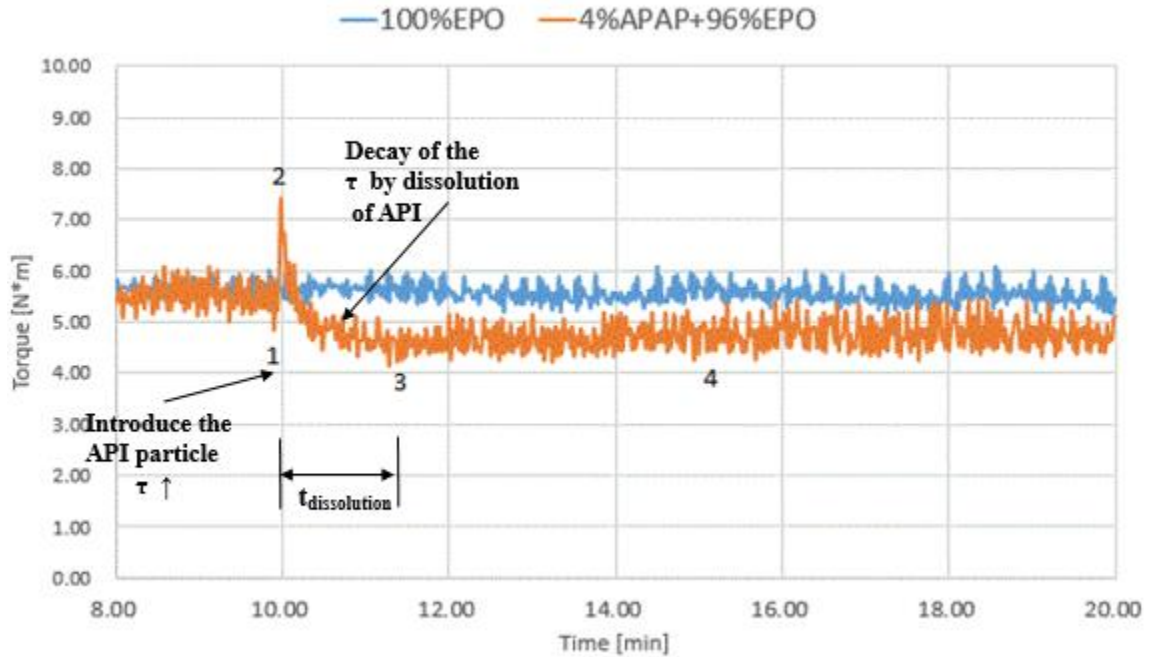


**Figure 3.2** 96%EPO-4%APAP vs. 100%EPO control.

Figure 3.2 compares the torque traces of pure EPO (control) and the sample containing 96%EPO-4%APAP. From the control sample, it can be seen that EPO has reached a steady state at ~8 min. And the polymer remains stable for another 12 min, allowing a processing window of 20 min, in which the material was melted and mixed. This allows the polymer to reach steady state, then the added API is dissolved, and finally the binary formulation reached steady state. From the torque tracer of the sample with the drug, we can see that the formulation also remains stable for ~8 min (after the addition of the API). In the sample with 4% API, the torque drop upon adding the drug was because the operator opened the cap of the mixer, so that the surface area of the stress decreased. The torque fluctuation before the point of the maximum torque after the addition of APAP, indicates the feeding surge, the wetting of the API particles surface and their dispersion and distribution in the molten polymer matrix. The final equilibrium torque is associated

with the apparent viscosity of the dissolved drug/polymer melt mixture in the mixing chamber.

The dispersion, distribution and dissolution of an API occur at the same time after the addition of the API in the molten polymer. To minimize the effect of dispersion and distribution of the API in the polymer matrix, we have kept the addition time and the amount of API added in the molten polymer was kept to a minimum. The evolution of the torque trace resulting from the addition of the API in the molten polymer can be used to approximate the amount of the API dissolved while it is dispersed and distributed in the molten polymer matrix. Figure 3.3 shows the relationship between the amount of dispersed API particle and the viscosity/torque increment.

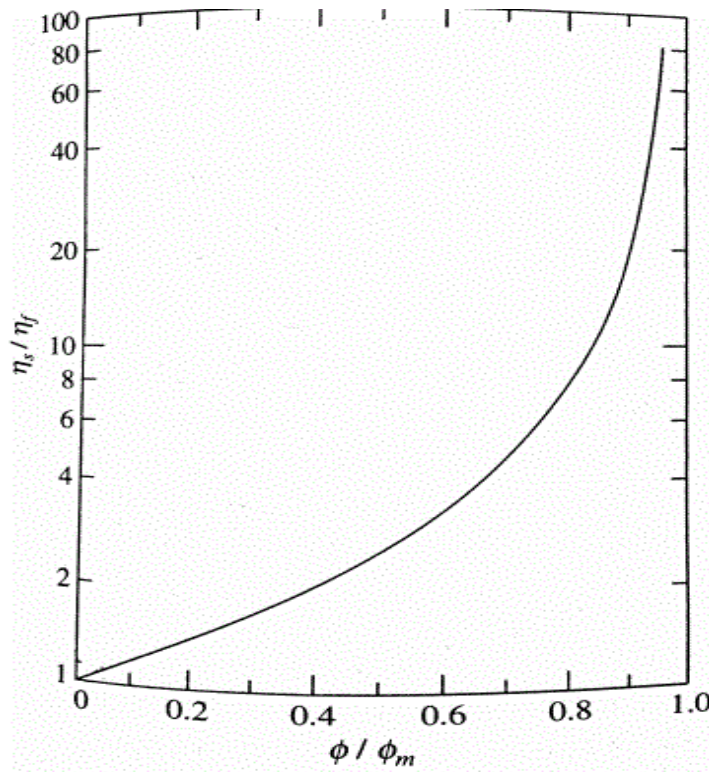


**Figure 3.3** Viscosity ratios of suspensions and viscosity ratios of suspended drug particles in molten polymer matrix.

Source: Bigg, D.M, Rheological Behavior of Highly Filled Polymer Melts, Society of Plastics Engineers, 1983.

The torque trace could be divided into the following parts: 1-2 is the part beginning with the addition of the drug and ending at the maximum value of torque recorded during after the drug is added. 2-3 is from the point where the torque is maximized until the drug fully dissolves. 3-4 is the steady state torque following the dissolution of the drug (respective points on Figure 3.2). The following “cartoon representation” of the evolving state of dispersive mixing and dissolution (Figure 3.4) is also used to help depict the phenomena occurring above:

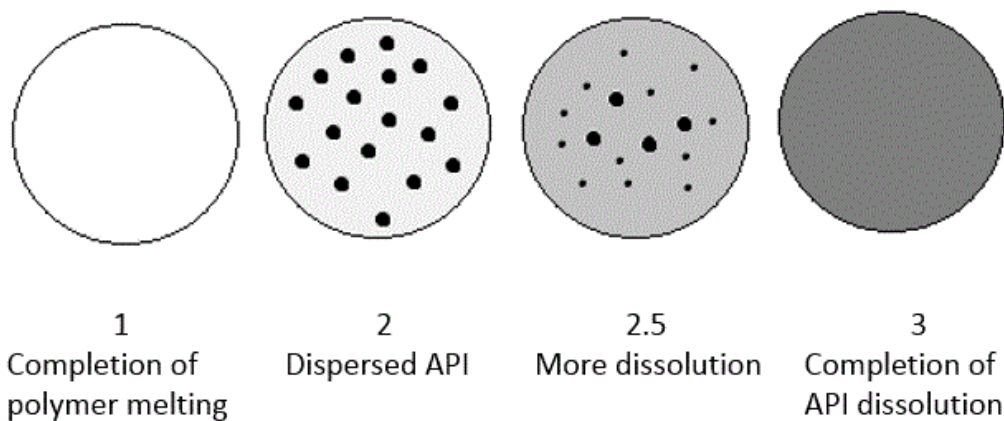


**Figure 3.4** Cartoon representation of the dissolution of APAP in molten EPO.

## 3.2 Dissolution of the API at Different Shear Rate

### 3.2.1 Shear Rate

In this work, the shear rate for different screw speeds can be calculated as equation (1.3), and the shear rates are 42/s, 84/s, 126/s and 168/s, corresponding to 25RPM, 50RPM, 75RPM, and 100RPM.

### 3.2.2 Exponential decay

Fang reported that the dissolution process can be expressed by an exponential decay function (Fang, 2014). Hence, the torque traces were fitted to exponential decay curves.

The expression is:

$$\tau = C_1 \times e^{-C_2 \cdot t} + \tau_0$$

Here  $\tau$  is torque in N/m;  $t$  is time in minute;  $C_1$  is pre-exponential-number;  $e$  is the base of the natural system of logarithms;  $C_2$  is the constant indicating the decay rate;  $\tau_0$  is the value of  $\tau$  at  $t \rightarrow \infty$ .

In this work, the API is considered to be completely dissolved when the total torque drops 99% of  $C_1$ , then the minimum time to complete the dissolution could be calculated:

$$C_1 + \tau_0 - 0.99C_1 = C_1 \times e^{-C_2 \cdot t} + \tau_0$$

The dissolution time  $t_d$ :

$$t_d = \frac{4.605}{C_2}$$

Due to the noise originated by the mixer, which was mentioned in Material and Method, repeated tests were conducted to filter the noise. After normalizing the time and taking the average torque at the same time point, the averaged torque traces at different conditions were obtained, shown as Figure 3.5.

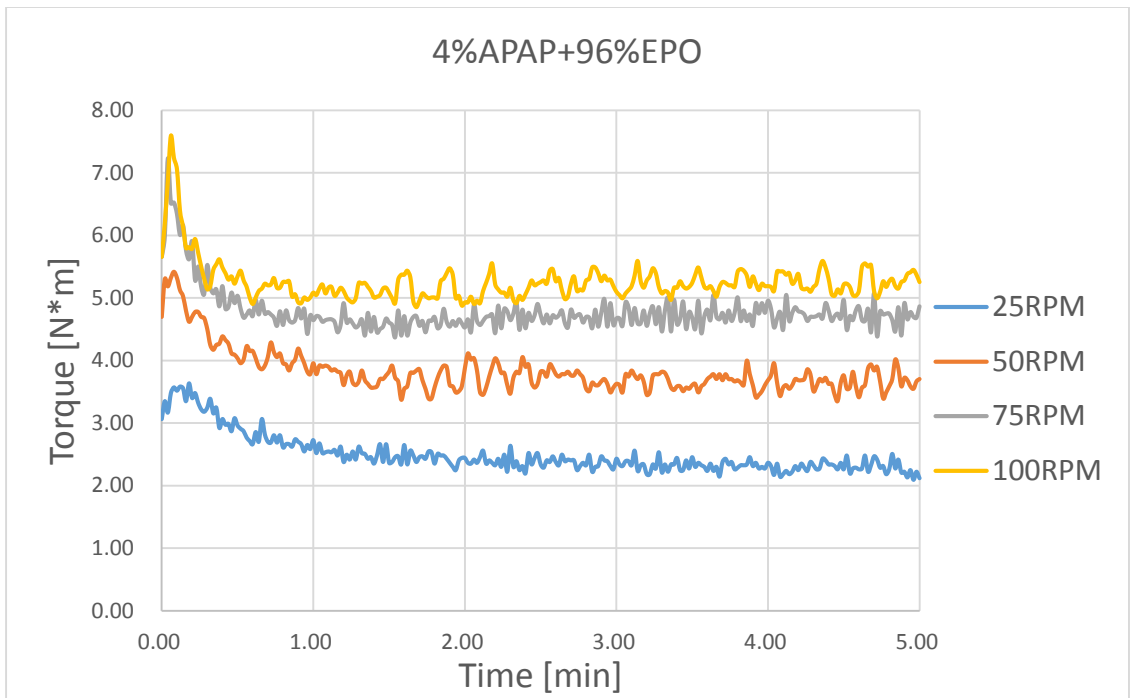


**Figure 3.5** Averaged torque traces with normalized time.

While fitting the torque traces into exponential decay curves, the torque peak and the torque at steady state were set as time zero and torque was normalized. All the torque traces are processed in this method. The exponential-decay curves are shown as Figure 3.6, and the constants and  $R^2$  of the functions are shown as Table 3.2.

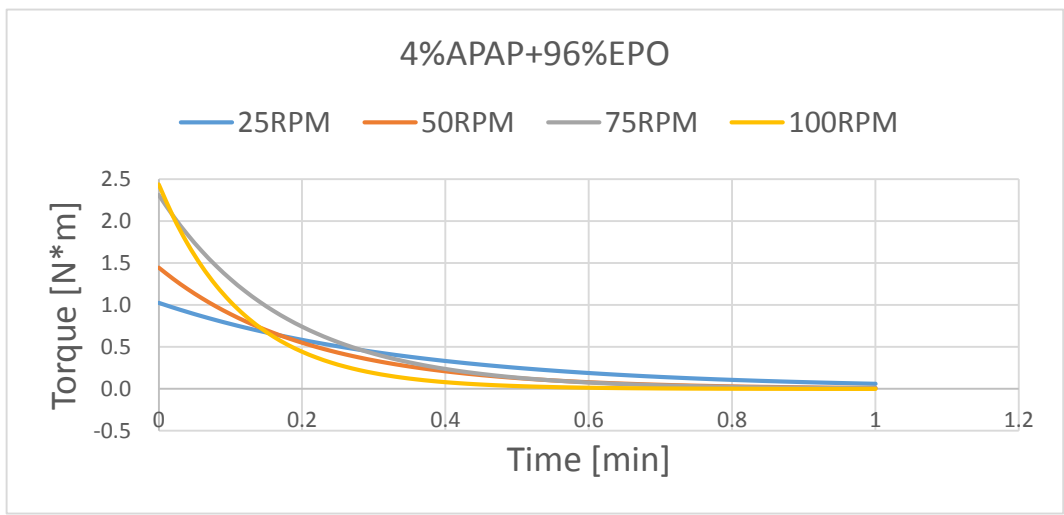


**Figure 3.6** Exponential decay curves after normalization.



**Table 3.2** Exponential Decay Model Parameters for 4% APAP at Different RPM

| RPM | $t_d/\text{min}$ | $C_1$  | $C_2$  | $\tau_0$ | $R^2$ |
|-----|------------------|--------|--------|----------|-------|
| 25  | 1.64             | 1.0254 | 2.8103 | 2.50143  | 0.9   |
| 50  | 1                | 1.4429 | 4.6083 | 3.92419  | 0.91  |
| 75  | 0.81             | 2.312  | 5.6841 | 4.68293  | 0.94  |
| 100 | 0.49             | 2.4355 | 9.4931 | 5.15348  | 0.92  |

The physical meaning of the parameters of the exponential decay function are as follows:  $C_1$  is the scaling factor of the decay function and corresponds to the value of the y-axis (torque) at  $t=0$ . In this case,  $C_1$  corresponds to the highest value of torque, which is proportional, for a given material stem and temperature, to the shear rate of the set RPM, following the addition, dispersion and distribution of the API in the polymer melt, and the initiation quantity of the API added (point 2 in Figure 3.4). According to “ $\tau = \gamma \times \eta$ ”,  $C_1$  is proportional to  $\gamma \times \eta$ , which means plotting the value of  $C_1$  vs. the shear rate yields a straight line, the slope depends on the dynamic viscosity, and it denotes the proportionality between the RPM and the corresponding increase in the torque of the melt.  $C_2$  in the exponential decay function indicates the decay rate of the material’s torque or viscosity due to the dissolution rate of the API. Higher value of  $C_2$  means polymer melt’s higher swiping effect on the surface of the API particle, which is proportional to the shear rate. Plotting the value of  $C_2$  vs. the set RPM yields another straight line, the slope of which denotes the proportionality between the RPM and the corresponding increase in the dissolution rate.  $\tau_0$  is the torque at  $t \rightarrow \infty$ . Similar reason as  $C_1$ ,  $\tau_0$  is proportional to  $\gamma \times \eta$ . It is also proportional to shear rate. Plotting the value of  $\tau_0$  vs. the set RPM yields another straight line.

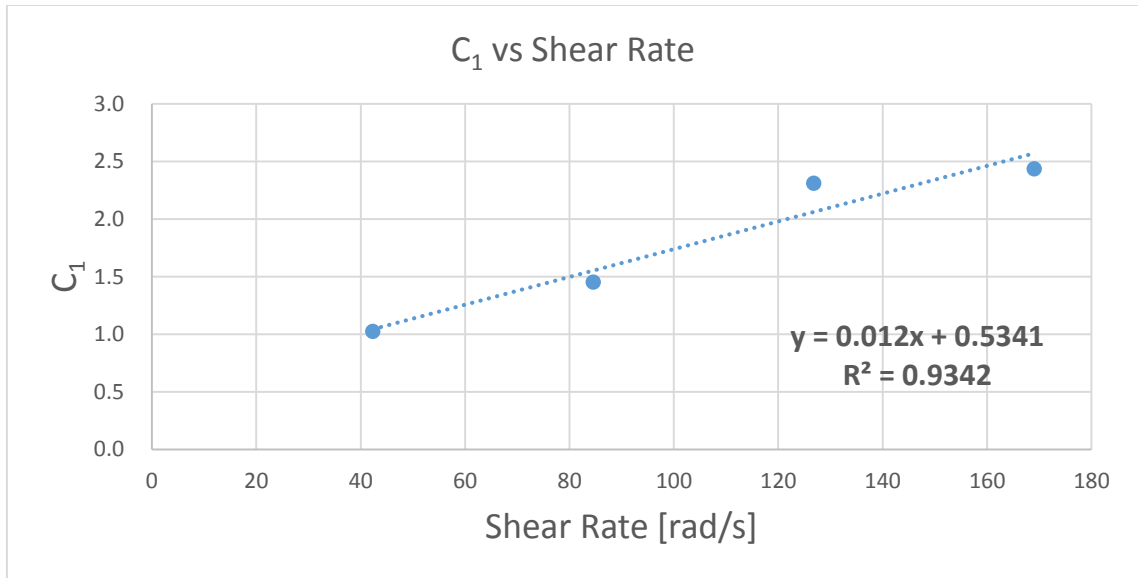


**Figure 3.7** C<sub>1</sub> vs Shear Rate.

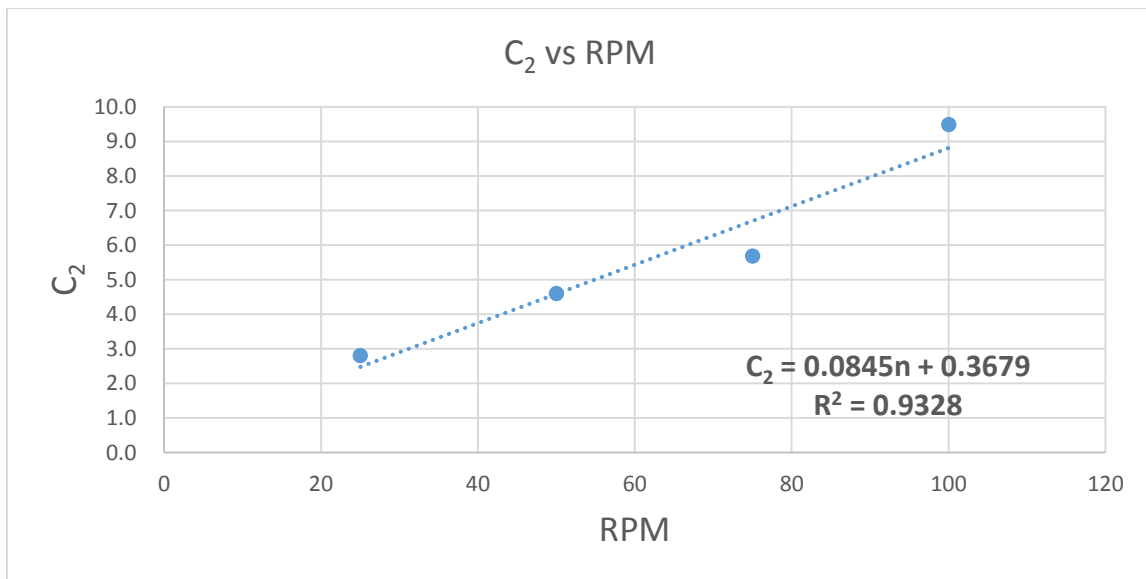


**Figure 3.8** C<sub>2</sub> vs RPM.

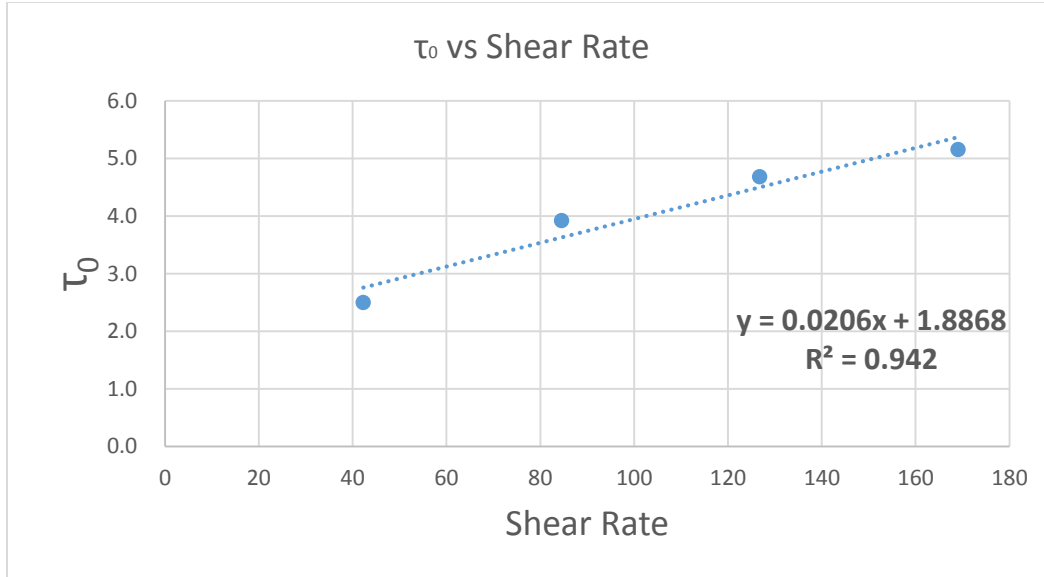


**Figure 3.9**  $\tau_0$  vs Shear Rate.

At the fixed API concentration and processing temperature, the torque can be expressed as below:

$$\tau = (0.0204n + 0.5341) \times \exp(-(0.0845n + 0.3679)t) + 0.035n + 1.8868 \quad (3.1)$$

For a given melt temperature, the dissolution kinetics is acquired. Now we consider that the dissolution is completed when the total torque drops 99%, then we have the dissolution time:

$$t_d = \frac{4.605}{0.0845n + 0.3679} \quad (3.2)$$

Equation 3.1 and 3.2 give the whole picture of the dissolution process and the guidance to minimize the residence time of an extruder for APAP/EPO system at 140 °C.

### 3.2.3 Drugs Concentration Effect

Figure 3.10 shows the torque traces corresponding to the dissolution process of the API into the molten polymer (points 2-4 in Figure 3.4) of formulations containing different amount of APAP at 50RPM and 100RPM. Also, the dissolution process is described as the following exponential decay function, which is:

$$\tau = C_1 \times e^{C_2 \cdot t} + \tau_0$$

And the exponential decay constants and  $R^2$  are shown in Table 3.3. The value of  $C_1$  is the pre-exponential factor, indicating the torque value at  $t=0$ , which is the max value of the torque. As it shows in Table 3.3,  $C_1$  is proportional to the concentration for both 50RPM and 100RPM. This is consistent with Fang's research (Fang 2014).

**Table 3.3** Exponential Decay Model Parameters for Different Condition and Formulation

| Condition         | $t_d$ /min | $C_1$  | $C_2$  | $\tau_0$ | $R^2$ |
|-------------------|------------|--------|--------|----------|-------|
| 4% APAP<br>50RPM  | 1.00       | 1.4528 | 4.6083 | 3.9242   | 0.92  |
| 8% APAP<br>50RPM  | 1.07       | 2.8507 | 4.2898 | 3.089    | 0.98  |
| 4% APAP<br>100RPM | 0.49       | 2.4355 | 9.4931 | 5.1535   | 0.91  |
| 8% APAP<br>100RPM | 0.65       | 4.7563 | 7.047  | 4.7563   | 0.96  |

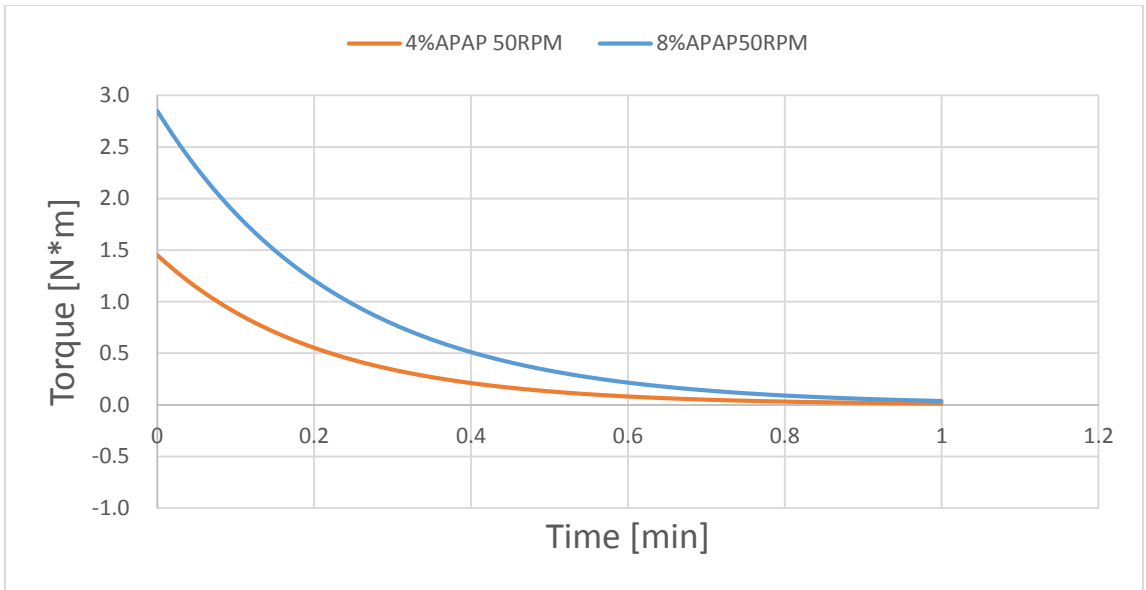


**Figure 3.10(a)** Torque trace at 50RPM.

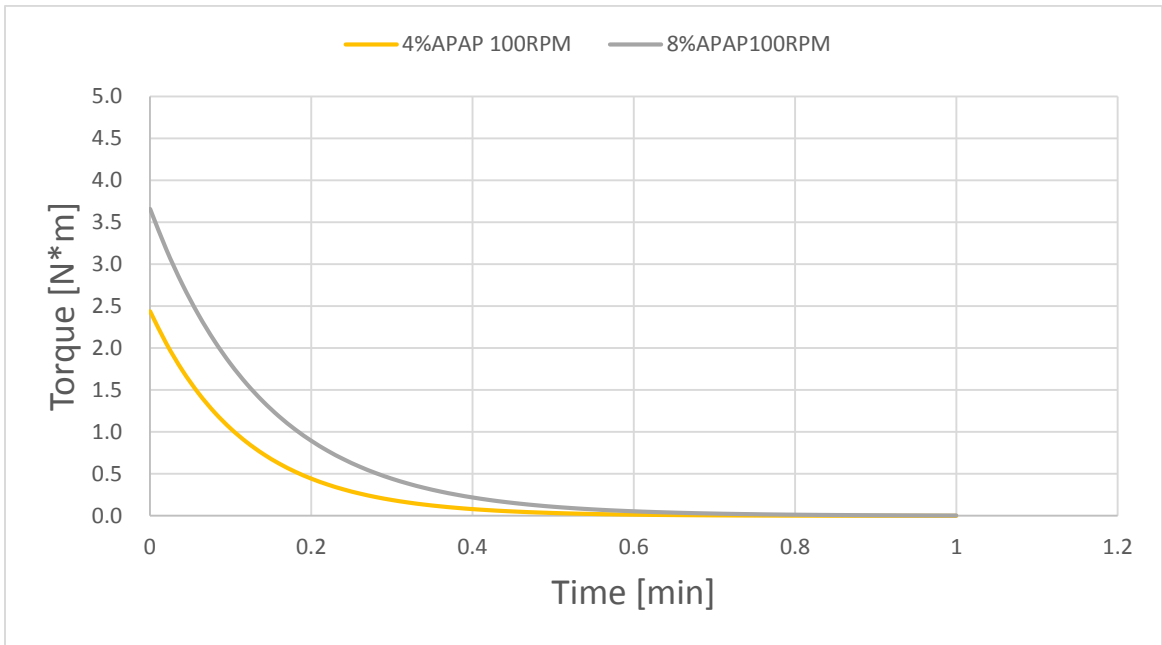


**Figure 3.10(b)** Torque trace at 100RPM.

### 3.2.4 Effect of API Species

Light microscopy was used to determine the particle size of two drugs, and Figure 3.11 shows that the APAP particle is slightly larger than the QTP particle but in same scale. This may lead to faster dissolution for QTP. On the contrary, the torque trace (Figure 3.12) shows that the dissolution rate of QTP is lower than that of APAP at the same concentration. The exponential factors are shown as Table 3.4.

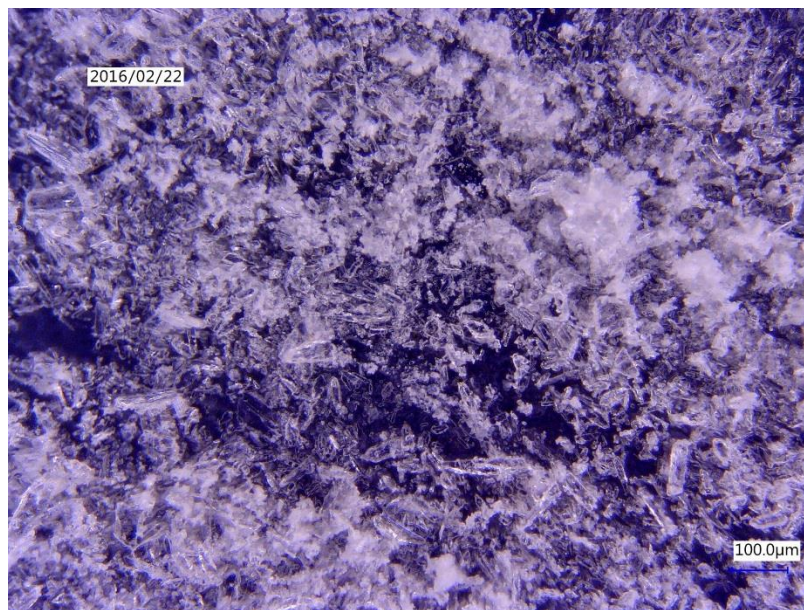


**Figure 3.11(a)** APAP particles.

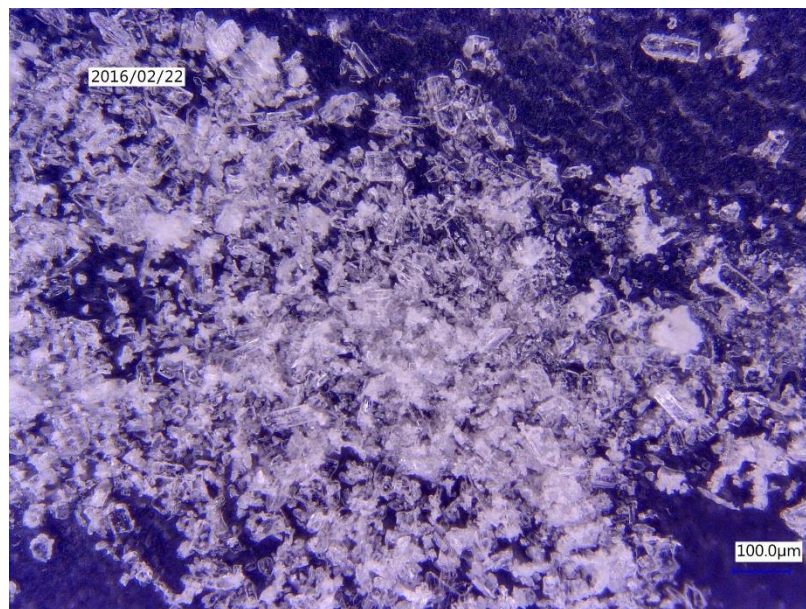


**Figure 3.11(b)** QTP particles.

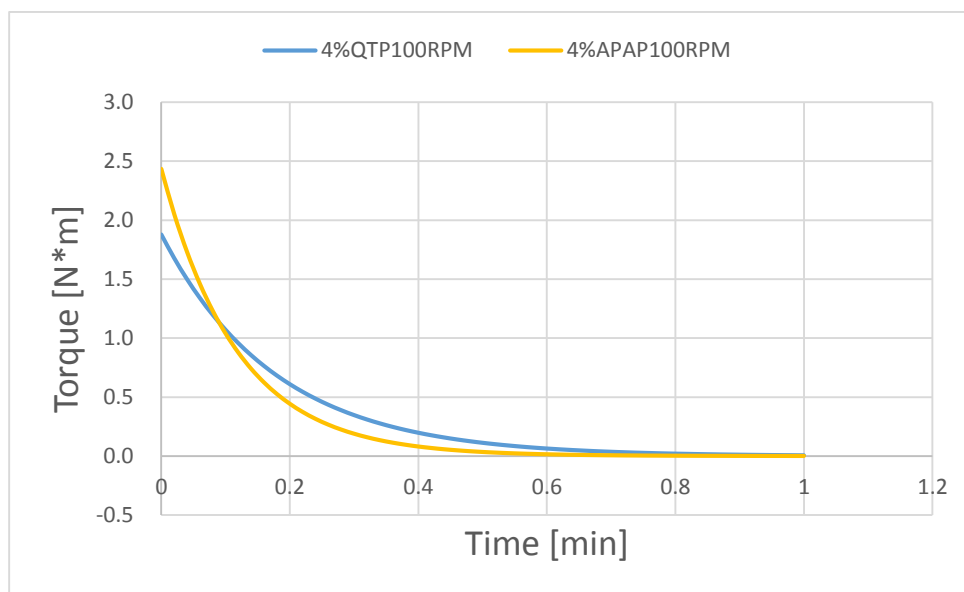


**Figure 3.12** Torque trace at 100RPM.

**Table 3.4** Exponential Decay Model Parameters for Different API

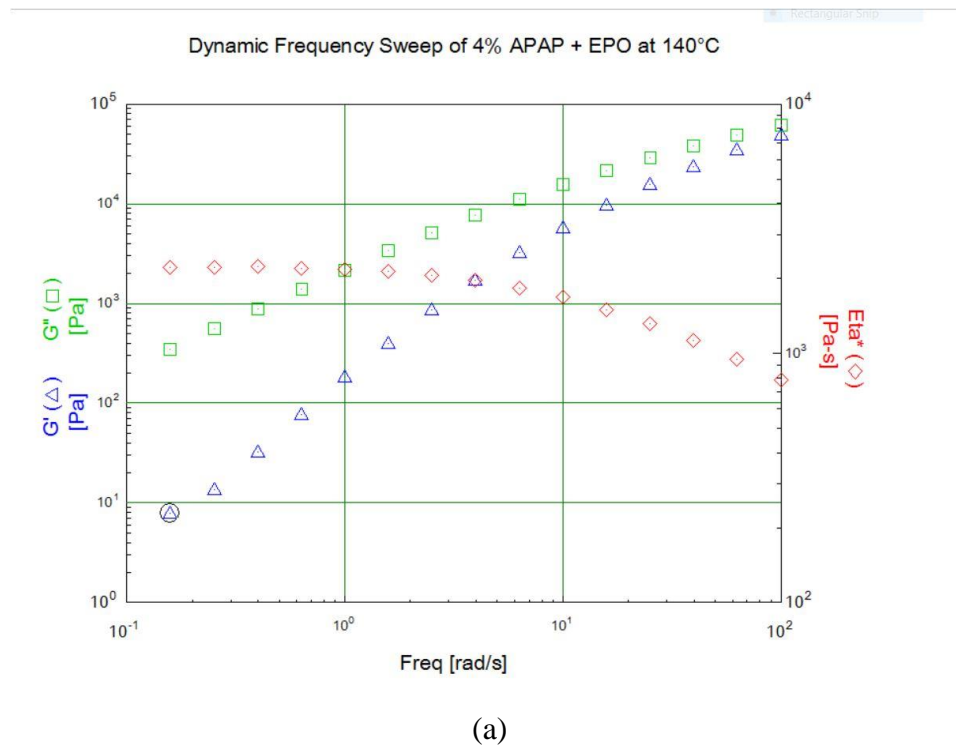
| Condition     | $t_d$ /min | $C_1$  | $C_2$  | $\tau_0$ | $R^2$ |
|---------------|------------|--------|--------|----------|-------|
| 4%APAP 100RPM | 0.49       | 2.4355 | 9.4931 | 5.1535   | 0.92  |
| 4%QTP 100RPM  | 0.65       | 1.8793 | 5.6192 | 5.2039   | 0.98  |

The particle sizes of QTP and APAP are of the same scale while QTP particle is slightly smaller than APAP particle. This may lead to higher dissolving rate. However, the experiment shows that at the same concentration and screw speed, the APAP dissolves faster than QTP. This indicates the stronger plasticization effect of APAP than QTP.

### 3.2.5 The Viscosity of the API/Excipient Systems at Different Shear Rate

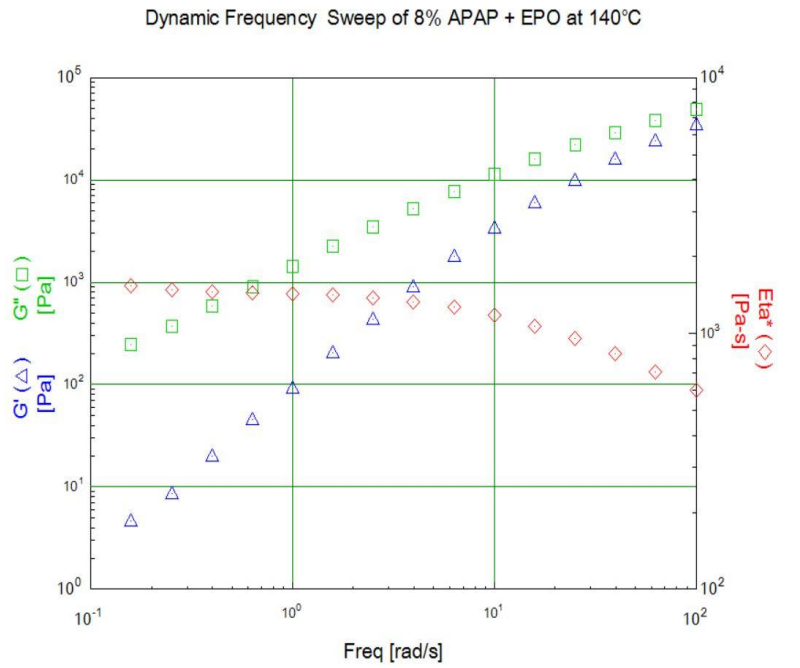
The characteristic channel shear rates are calculated by Equation (1.3), and they are 42/s, 84/s, 126/s and 168/s, corresponding to 25RPM, 50RPM, 75RPM, and 100RPM.

Figure 3.13 shows the rheology results of three API/Excipient melts systems at 140°C: 4% APAP + 96% EPO, 8% APAP + 92% EPO and 4% QTP + 96% EPO:

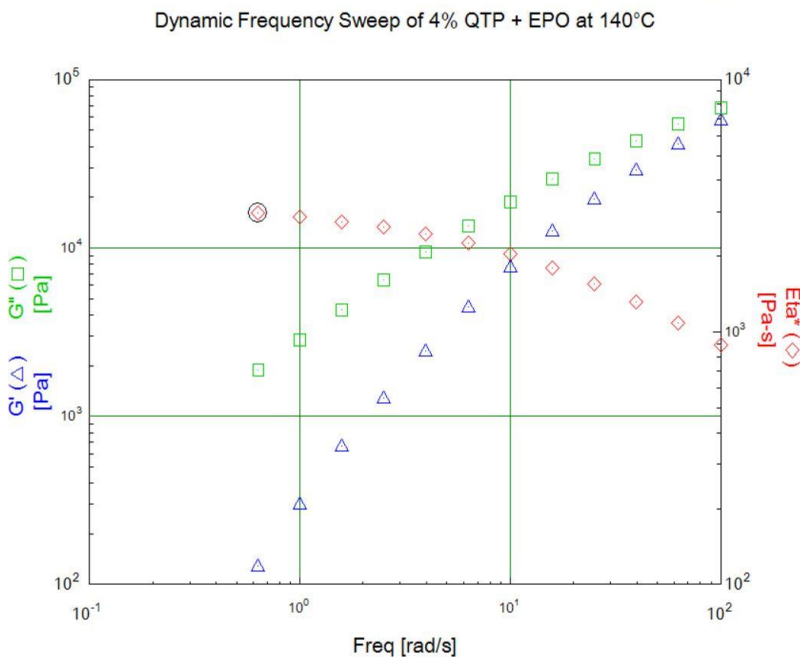


**Figure 3.13** Rheology results at 140°C of: (a) 4% APAP + 96% EPO.



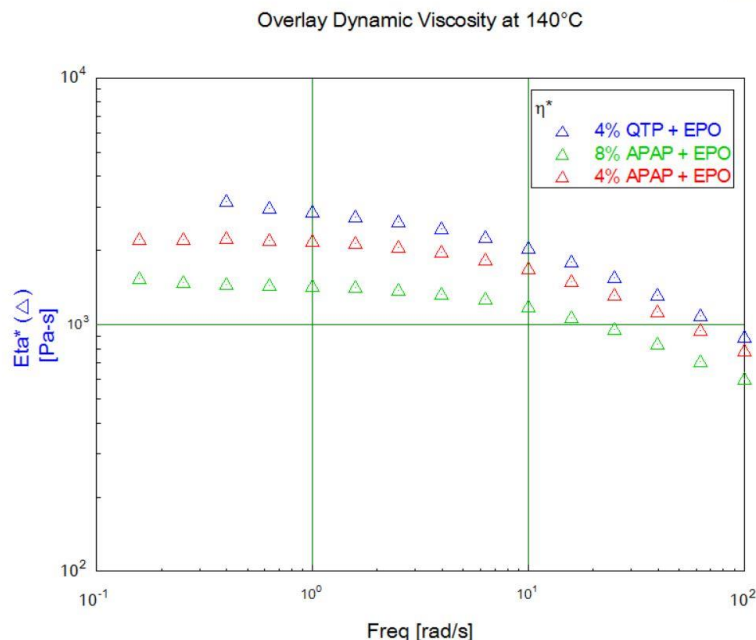


(b)



(c)

**Figure 3.13** Rheology results at 140°C of: (b) 8% APAP + 92%, (c) 4% QTP + 96% EPO.



(d)

**Figure 3.13** Rheology results at 140°C of: (d) Summary of dynamic viscosities of the three API/EPO systems. Note that the frequency of the oscillatory shear deformation is taken to be the same as the shear rate in laminar flows, such as that in the Brabender batch mixer.

Examining the rheology results, at 140°C, all of the samples show that  $G'$  (viscous modulus) is always higher than  $G''$  (elastic modulus) at all frequencies, indicating the predominant viscous nature of all the samples at this temperature. Furthermore, the samples behave like Newtonian fluids at frequencies lower than 1 rad/s. They have a non-Newtonian nature for all the Brabender shear mixing flows, employed in this work, which are in the range of 40-170 Rad/s. Additionally, both the concentration and the API species have an effect on dynamic viscosity. Figure 3.13 (d) indicates that the viscosity drops with the increasing concentration of APAP. That is because the API acts as a plasticizer and the plasticization effects increases with the rising of the API concentration. As for the two different API species, the APAP particles has a stronger plasticization effect than QTP

particles. This is caused by the stronger molecular interaction force between APAP and EPO, compared to the interaction between QTP and EPO.

Due to the limited shear rate range, the dynamic viscosity data requires extrapolation. The raw data was fit to the function as shown in Figure 3.14, and the results are shown in Table 3.5:

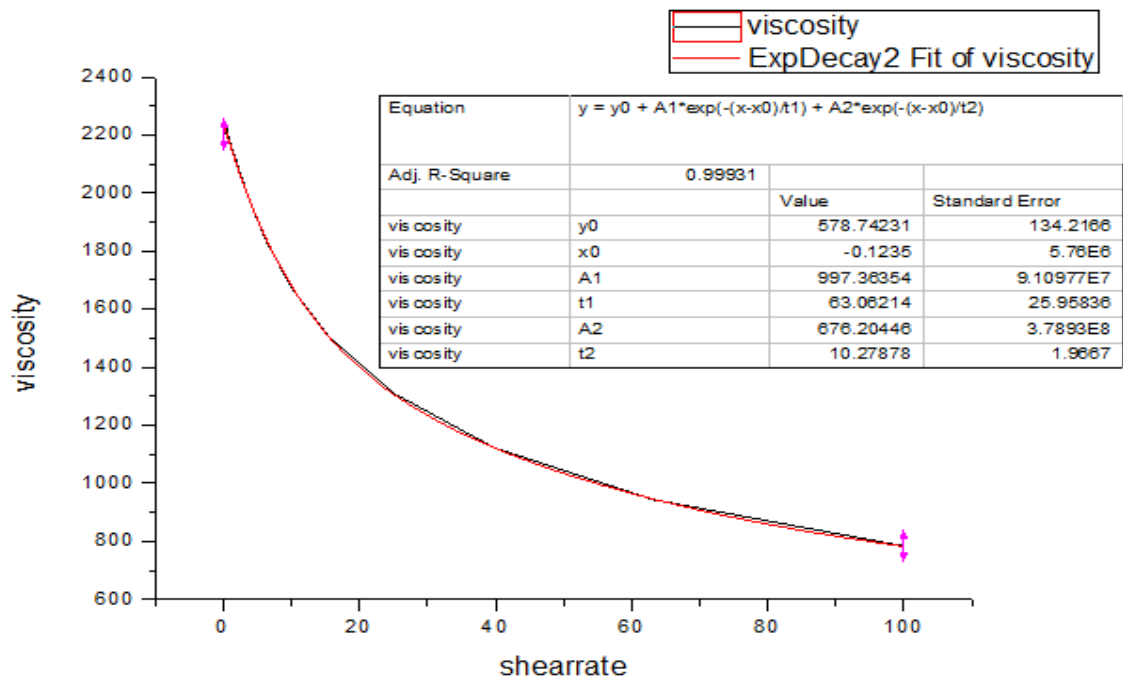


**Figure 3.14** Dynamic viscosity data analysis.

**Table 3.5** Dynamic Viscosities at Given Shear Rates

|            |           |           |          |          |
|------------|-----------|-----------|----------|----------|
| RPM        | 25        | 50        | 75       | 100      |
| Shear Rate | 42/s      | 84/s      | 126/s    | 168/s    |
| Viscosity  | 1309 Ps*s | 1034 Ps*s | 882 Ps*s | 783 Ps*s |

Recall that  $\tau = \gamma \times \eta$ , and  $C_1$  is proportional to  $\gamma \times \eta$ . Here the proportional relationship is verified:

**Table 3.6** Calculation of " $\gamma_i \times \eta_i$ "

| RPM | $\gamma / \text{Rad} \cdot \text{s}^{-1}$ | $\eta / \text{Pa} \cdot \text{s}$ | $\eta \cdot \gamma$ | $(\eta_i \cdot \gamma_i) / (\eta_1 \cdot \gamma_1)$ | $C_1$ | $C_i / C_1$ |
|-----|---|-----------------------------------|---------------------|---|-------|-------------|
| 25  | 42  | 1309                              | 54978               | 1   | 1.03  | 1           |
| 50  | 84  | 1034                              | 86856               | 1.58  | 1.44  | 1.4         |
| 75  | 126                                       | 882                               | 111132              | 2.02  | 2.31  | 2.22        |
| 100 | 168                                       | 783                               | 131544              | 2.39  | 2.44  | 2.37        |

The value of  $(\eta_i \cdot \gamma_i) / (\eta_1 \cdot \gamma_1)$ ,  $C_1$  and  $C_i / C_1$  are closed, which shows  $C_1$  is proportional to  $\gamma \times \eta$ .

Referring the solubility parameter gives us more information on this: using the group contribution method (Van Krevelen, 1976; Hansen, 2007; Just et al. 2013),

$$\delta = \sqrt{\delta_d^2 + \delta_p^2 + \delta_h^2}$$

where:

$$\delta_d = \frac{\sum F_{di}}{V}$$

$$\delta_p = \frac{\sqrt{\sum F_{pi}^2}}{V}$$

$$\delta_h = \frac{\sqrt{\sum E_{hi}}}{V}$$

Here  $\delta$  is the total solubility parameter;  $\delta_d$  is the contribution from dispersion forces;  $\delta_p$  is the contribution from polar forces;  $\delta_h$  is the contribution from hydrogen bonding;  $F_{di}$  is the molar attraction constant from dispersion component;  $F_{pi}$  is the molar

attraction constant from polar component;  $E_{hi}$  is the hydrogen bonding energy;  $V$  is the molar volume.

**Table 3.7** Solubility Parameter Calculation of EPO

| Functional groups   | $F_{di}$<br>( $J^{1/2} \cdot cm^{3/2} \cdot mol^{-1}$ ) | $F_{pi}$<br>( $J^{1/2} \cdot cm^{3/2} \cdot mol^{-1}$ ) | $E_{hi}$<br>( $J \cdot mol^{-1}$ ) |
|---------------------|---|---|------------------------------------|
| 9 -CH <sub>3</sub>  | 336.6   | 0   | 0                                  |
| 4 >C<               | -214.2  | 0   | 0                                  |
| -N<                 | 30.0  | 150.0   | 750.0                              |
| 4-COO-              | 204.0   | 450.0   | 12500.0                            |
| 9-CH <sub>2</sub> - | 234.6   | 0   | 0                                  |
| Molar Volume        | 453.64 cm <sup>3</sup> /mol                             |   |                                    |
|                     | $\delta_d=11.31MPa^{1/2}$                               | $\delta_p=2.01MPa^{1/2}$                                | $\delta_h=10.58MPa^{1/2}$          |
| Total               | $\delta=15.62MPa^{1/2}$                                 |   |                                    |

**Table 3.8** Solubility Parameter Calculation of APAP

| Functional groups | $F_{di}$<br>( $J^{1/2} \cdot cm^{3/2} \cdot mol^{-1}$ ) | $F_{pi}$<br>( $J^{1/2} \cdot cm^{3/2} \cdot mol^{-1}$ ) | $E_{hi}$<br>( $J \cdot mol^{-1}$ ) |
|-------------------|---|---|------------------------------------|
| Phenylene         | 1173.0  | 63.7  | 40.4                               |
| -OH Phenylge      | 51.0  | 1300.0  | 12000.0                            |
| -CO-NH-           | 225.0   | 400.0   | 4000.0                             |
| -CH <sub>3</sub>  | 336.6   | 0   | 0                                  |
| Molar Volume      | 119.97 cm <sup>3</sup> /mol                             |   |                                    |
|                   | $\delta_d=14.88MPa^{1/2}$                               | $\delta_p=11.34MPa^{1/2}$                               | $\delta_h=13.86MPa^{1/2}$          |
| Total             | $\delta=23.28MPa^{1/2}$                                 |   |                                    |

**Table 3.9** Solubility Parameter Calculation of QTP

| Functional groups     | $F_{di}$<br>( $J^{1/2} \cdot cm^{3/2} \cdot mol^{-1}$ ) | $F_{pi}$<br>( $J^{1/2} \cdot cm^{3/2} \cdot mol^{-1}$ ) | $E_{hi}$<br>( $J \cdot mol^{-1}$ ) |
|-----------------------|---|---|------------------------------------|
| 4 Phenylene           | 1173.0  | 63.7  | 40.4                               |
| 2 -S-                 | 815.9   | 196.0   | 297.5                              |
| 2 -N=                 | 380.0   | 100.0   | 250.0                              |
| 4 -N<                 | 30.0  | 150.0   | 750.0                              |
| 2=C<                  | -56.7   | 20.0  | 0                                  |
| 4 Ring5-              | 142.8   | 0   | 0                                  |
| 16 -CH <sub>2</sub> - | 234.6   | 0   | 0                                  |
| 2 -O-                 | 76.5  | 1225.0  | 101.0                              |
| 2 -OH                 | 76.5  | 1225.0  | 6060.0                             |
| 2 -COOH               | 561.0   | 833.0   | 14645.0                            |
| 2-CH=                 | 255.0   | 38.0  | 0                                  |
| Molar Volume          | 630.79cm <sup>3</sup> /mol                              |   |                                    |
|                       | $\delta_d=21.16MPa^{1/2}$                               | $\delta_p=4.37MPa^{1/2}$                                | $\delta_h=8.53MPa^{1/2}$           |
| Total                 | $\delta=23.24MPa^{1/2}$                                 |   |                                    |

The solubility parameters of APAP, QTP and EPO are  $23.28MPa^{1/2}$ ,  $23.24MPa^{1/2}$  and  $15.62MPa^{1/2}$ . The solubility parameter difference between API and excipient is an indicator on the miscibility of the system: a system with less than  $7MPa^{1/2}$  difference is generally considered as miscible whereas a system with more than  $10 MPa^{1/2}$  difference is unlikely to be miscible (Chokshi et al. 2005). The solubility parameter difference between APAP/QTP and EPO is  $7.6\sim 7.7MPa^{1/2}$ , which is in the lower end of the miscibility/immiscibility limit range. The solubility parameter difference between APAP and EPO ( $7.66$ ), compared to that between QTP and EPO ( $7.62$ ) indicates the approximately same molecular interaction force in two systems. This is not consistent with

the data of the batch mixing experiments. Then, the experimentally observed faster dissolution rate of APAP is indicative that one cannot make a strong correlation between the solubility parameter difference and dissolution rate, although the solubility parameter helps to predict the miscibility of a given system.

## CHAPTER 4

### SUMMARY, CONCLUSIONS, AND FUTURE WORK

#### 4.1 Summary

In this work, we used a batch mixer, light microscopy and rheometric mechanical spectroscopy to determine the dissolution kinetics of two model APIs and a polymer during Hot-melt extrusion, under different shear rates. Acetaminophen (APAP) and Eudragit® E PO (EPO) were selected as the model API/polymer system. In a limited range of cases, quetiapine fumarate (QTP) was used as a second model API.

For batch mixing experiments, a series of calibration mixing runs were performed to determine the processing temperature as a function of the shear rate. This allowed us to run the actual laminar flow dissolution runs at different barrel set temperatures that resulted in the same melt temperature at different shear rates. In addition, to minimize the effect of the dispersion of the API in the polymer, the latter was first melt-mixed, then only a small API quantity was added to the melt minimizing the chances of API particulate agglomeration. In this way, the resulting modest but easily measurable torque changes following the addition of the API, were only associated with the dissolution of the API. Analysis of the raw torque trace data, yielded the expression of the model API dissolution at 140°C. The dissolution rate of APIs in polymer excipients was found to be exponentially decaying with time after the addition of the API particulates characterized by three different decay function parameters,  $C_1$ ,  $C_2$  and  $\tau_0$ .  $C_1$  is the scaling factor of the decay function and corresponds to the value of the y-axis (torque) at  $t=0$ .  $C_2$  in the exponential decay function



indicates the decay rate of the material's torque or viscosity due to the dissolution rate of the API. As 99% of torque drop was considered as completion of dissolution, the dissolution time is determined as:  $t_d = \frac{4.605}{c_2} \tau_0$ .  $\tau_0$  is the torque at  $t \rightarrow \infty$ , which is the torque after complete dissolution.

Also, the effect of concentration on the dissolution rate was examined. By conducting the same operation on the APAP/EPO system with different API concentration, the dissolution rate expression was determined, showing that  $C_1$  is proportional to the concentration at the same shear rate.

In addition, the effect of chemical structure of the API on its dissolutions kinetics was examined by replacing APAP with QTP. While QTP particle size is smaller than that of APAP, at the same concentration, temperature and shear rate, the dissolution rate of QTP is lower than that of APAP, which means the intermolecular interactions of the EPO/APAP system is stronger than in the EPO/QTP system.

RMS experiments were conducted to find the viscoelastic nature of the API/polymer systems and the direct relationship between shear rate and viscosity. The results are consistent with the result of previous batch experiments: the viscosity drops with the increasing concentration of APAP and the dissolved APAP molecules have a stronger interaction (plasticization effect) with EPO than QTP molecules.

Equations 3.1, equation 3.2 and the specific values of the parameters for the APAP/EPO API/polymer excipient system can be used to determine the Hot-melt Extrusion (HME) minimum residence times, which will guarantee the complete dissolution of the API while minimizing the degradation concern during HME. This reduces the need

of costly and time-consuming extruder experiments. This work represents a valuable methodology of specifying the HME process “operating window” for any API/Polymer excipient system.

In the future, we expect a universal expression of dissolution rate to be developed. Ideally, for a given API/Polymer excipient system, the dissolution rate could be expressed as a function of all conditions: screw speed, set temperature and API concentration. Moreover, more API/Polymer excipient systems are to be examined to give a guidance to HME engineers in industrial practice.

## REFERENCES

- M. Maniruzzaman, J. S. Boateng, M. J. Snowden, and D. Douroumis, "A Review of Hot-melt Extrusion: Process Technology to pharmaceutical Products," *ISRN Pharmaceutics*, vol. 2012, 9 pages, 2012.
- G. P. Andrews and D. S. Jones, "Formulation and characterization of hot melt extruded dosage forms: challenges and opportunities," *Cheminform*, vol. 41, No. 43, 2010.
- M. M. Crowley, F. Zhang, M. A. Repka et al., "Pharmaceutical applications of hot-melt extrusion: part I," *Drug Development and Industrial Pharmacy*, vol. 33, No. 9, pp. 909–926, 2007.
- J. Breitenbach, "Melt extrusion: from process to drug delivery technology," *European Journal of Pharmaceutics and Biopharmaceutics*, vol. 54, No. 2, pp. 107–117, 2002.
- R. Chokshi and H. Zia, "Hot-melt extrusion technique: a review," *International Journal of Pharmaceutical Research*, vol. 3, pp. 3–16, 2004.
- J. W. McGinity and J. J. Koleng, "Preparation and evaluation of rapid release granules using novel melt extrusion technique," *American Association of Pharmaceutical Scientists*, pp. 153–154, 2004.
- D. S. Jones, "Engineering drug delivery using polymer extrusion/ injection moulding technologies," *School of Pharmacy*, vol. 4-9, pp. 18–27, 2008.
- H. H. Grunhagen and O. Muller, "Melt extrusion technology," *Pharmaceutical Manufacturing International*, vol. 1, pp. 167–170, 1995.
- S. Singhal, V. K. Lohar, and V. Arora, "Hot-melt extrusion technique," *WebmedCentral Pharmaceutical Sciences*, vol. 2, No. 1, Article ID 001459, 2011.
- Z. Tadmor, C.G. Gogos, "*Principles of Polymer Processing*," Wiley, Hoboken, NJ, USA, 2<sup>nd</sup> edition, 2006
- C.G. Gogos, H. Liu, P. Wang, in: Douroumis, "*Hot-Melt Extrusion: Pharmaceutical Applications*," Wiley, Chichester, UK, 2012
- Liu, H. (May 2010) *Hot Melt Mixing/Extrusion and Dissolution of Drug (Indomethacin) in Acrylic Copolymer Matrices*. Otto H. York Department of Chemical, Biological and Pharmaceutical Engineering. Newark, New Jersey Institute of Technology. Ph.D. Dissertation.
- Nollenberger and Albers, in: Douroumis, "*Hot-Melt Extrusion: Pharmaceutical Applications*," Wiley: Chichester, UK, 2012

- Gohel and Patel, "Compatibility study of quetiapine fumarate with widely used sustained release excipients," *Journal of Thermal Analysis and Calorimetry*, pp. 2103–2108, 2013.
- G. Garbacz, A. Kandzi, M. Koziolok, J. Mazgalski, and W. Weitschies, "Release Characteristics of Quetiapine Fumarate Extended Release Tablets under Biorelevant Stress Test Conditions," *AAPS PharmSciTech*, Vol. 15, No.1, 2014
- I. Ghebre-Sellassie, and C. Martin, "Pharmaceutical Extrusion Technology." *Informa Healthcare*, 2007
- D.M. Bigg, "Rheological Behavior of Highly Filled Polymer Melts," *Society of Plastics Engineers*, 23, 206, 1983
- H. Fang (May 2014), *The Kinetics of Drugs Dissolution in Polymer by Hot Melt Extrusion*, Otto H. York Department of Chemical, Biological and Pharmaceutical Engineering. Newark, New Jersey Institute of Technology. MS Thesis
- D.W. Van Krevelen, "*Properties of Polymer*," Elsevier Scientific Publishing Company, Amsterdam, Netherland, 2<sup>nd</sup> edition. 1976
- C.M. Hansen, "*Hansen Solubility Parameters: A User's Book*", CRC Press, Boca Raton, 2<sup>nd</sup> edition, 2007
- S. Just, F. Sievert, M. Thommes and J. Breitzkreutz, "Improved Group Contribution Parameter Set for the Application of Solubility Parameters to Melt Extrusion," *European Journal of Pharmaceutics and Biopharmaceutics*, Volume 85, Issue 3, Part B, 2013
- R.J. Chokshi, H.K. Sandhu, R.M. Iyer, N.H. Shah, A.W. Zia, "Characterization of Physico-Mechanical Properties of Indomethacin and Polymers to Assess their Suitability for Hot-Melt Extrusion Process as a Means to Manufacture Solid Dispersion/Solution," *Journal of Pharmaceutical Sciences*, Volume 94, Issue 11, pp. 2463–2474, 2005